

**STUDY OF COMPARISON IN CORROSION RESISTANCE
OF FRICTION STIR WELDING ALUMINUM ALLOY
(AA6061 AND AA1100)**

By

AJMAL FALIQ BIN JAMAL
11432

Dissertation submitted in partial fulfillment of
the requirements for the
Bachelor of Engineering (Hons)
(Mechanical Engineering)

MAY 2012

Universiti Teknologi PETRONAS
Bandar Seri Iskandar
31750 Tronoh
Perak Darul Ridzuan

CERTIFICATION OF APPROVAL

**STUDY OF COMPARISON IN CORROSION RESISTANCE
OF FRICTION STIR WELDING ALUMINUM ALLOY
(AA6061 AND AA1100)**

By

AJMAL FALIQ BIN JAMAL

A project dissertation submitted to the
Mechanical Engineering Program
Universiti Teknologi PETRONAS
in partial fulfillment of the requirement for the
Bachelor of Engineering (Hons)
(Mechanical Engineering)

Approved by,

(HAJI KAMAL ARIFF BIN ZAINAL ABIDIN)

UNIVERSITI TEKNOLOGI PETRONAS

TRONOH, PERAK

MAY 2012

CERTIFICATION OF ORIGINALITY

This is to certify that I, Ajmal Faliq Bin Jamal (I/C No: 900111-01-5509), am responsible for the work submitted in this project, that the original work is my own except as specified in the references and acknowledgements, and that the original work contained herein have not been undertaken or done by unspecified sources or persons.

AJMAL FALIQ BIN JAMAL

Student ID : 11432

I/C No : 900111-01-5509

Date : 11th AUGUST 2012

ACKNOWLEDGEMENT

First and above all, praises and thanks to Allah, for His showers of blessings throughout my research work to complete in the desired timeline. Without the blessing from the Almighty, this project will not be accomplished as it stands. I wish to express my sincere gratitude to my Final Year Project supervisor, Haji Kamal Ariff Bin Zainal Abidin, senior lecturer of Mechanical Engineering Department of Universiti Teknologi Petronas for providing me an opportunity to do my project work on "Comparison on Corrosion Resistance of Friction Stir Welding Aluminum Alloy (AA1100 and AA6061)". This research project would not have been possible without the support of my respected supervisor.

I would also want to thank all lecturers, technicians, and staffs of Mechanical Engineering and Centre for Corrosion Research Department for their co-operations, suggestions and time responding to my inquiries along the way. Deepest thanks and appreciation to my beloved parents, En Jamal Bin Tuminok and Pn Faridah Binti Jailani and family for their love, support and prayers during my time on completing this project.

Not to forget, to all my friends and work mate especially for their cooperation, encouragement, constructive suggestion and full of support for this project completion, from the beginning till the end. Thanks to everyone who has been contributing by supporting my work during the final year project progress till it is fully completed.

ABSTRACT

Friction stir welding is an alternative option of joining process that use the idea of frictional heat to soften a stirred materials without the need of melting. This study is focusing in the comparison of the corrosion resistance and microstructure properties between friction stir welded AA6061 and AA1100 Aluminum Alloy. These microstructures suggested to be characterized by the mean of optical microscopy (OM) and Field Emission Scanning Electron Microscopy (FESEM) to oversee any finding on creation of pitting prior to the corrosion testing. The location of selective intergranular attack relative to the welding nugget following the 24 hour exposure to ASTM G-34 modified solution can be illustrated by low magnification optical micrograph. The observation on the corrosion current (I_{corr}) properties suggested to be studied in 3% NaCl solution at a constant temperature of 30°C (room temperature). These microstructures corrosion resistance can been examined and differentiate by four (4) different zones of friction stir welding process; base metal zone, thermo – mechanically affected zone (TMAZ), weld nugget zone and heat affected zone (HAZ).

TABLE OF CONTENT

1.0	Introduction		
	1.1	Background of Study	1
	1.2	Problem Statement	2
		1.2.1 Problem Identification	2
		1.2.2 Significant of the Project	2
	1.3	Objectives	3
	1.4	Scope of Study	3
	1.5	Relevancy of Project	4
	1.6	Feasibility of Project	4
2.0	Theory and Literature Review		5
	2.1	The ideas of Friction Stir Welding	5
	2.2	The process of Friction Stir Welding	6
	2.3	FSW Microstructural Zones	8
	2.4	FSW Tool Design	10
	2.5	Corrosion Perception View	11
	2.6	Corrosion Mechanism	12
		2.6.1 Oxide Destabilization	12
		2.6.2 Pitting	12
		2.6.3 Intergranular Corrosion Attack	13
3.0	Methodology		14
	3.1	Task Workflow	14
	3.2	Project Milestones and Gantt Chart	15
	3.3	Material Selection for Specimen and Tool	17
	3.4	Fabrication of FSW Tool	18
	3.5	Heat Treatment of AISI H13 Tool	20
	3.6	Friction Stir Welding Process	22
	3.7	Sample Preparation for Microstructure Scanning	23

		3.7.1 Specimen Sizing and Standard	23
		3.7.2 Grinding and Polishing	23
		3.7.3 Etching	24
	3.8	Sample Preparation for Corrosion Tests	25
		3.8.1 Electrochemical Cell	25
		3.8.2 Sample Preparation for Corrosion	26
4.0	Result and Discussion		27
	4.1	Friction Stir Welding Result	27
	4.2	Defects on the FSW Aftermath Process	28
		4.1.2 Sensitivity analysis for pipeline (single phase gas)	32
	4.3	Effects on Tool Pin Profile	30
	4.4	Microstructure Examinations on different conditions	32
	4.5	Microstructure and Pitting Observation via Field Emission Scanning Electron Microscope (FESEM)	33
	4.6	Mapping Analysis	36
	4.7	Susceptibility to Intergranular Attack Study	37
	4.8	Potentiostatic Polarization Measurement via Tafel Extrapolation	39
5.0	Conclusion and Recommendation		43
	References		45
	Appendices		48

LIST OF FIGURES

No	Figure Name	Page
Figure 2.1	Schematic of FSW Process	6
Figure 2.2	FSW Process Material Ending Product	7
Figure 2.3	Cross sectional Area of the Material with respect to Microstructural Zones	8
Figure 2.4	Advancing and Retreating Side of FSW	9
Figure 2.5	FSW tool basic dimensions	10
Figure 2.6	Key Design of the FSW Tool Pin Profiles	10
Figure 2.7	Generalized illustration of pitting corrosion on aluminum alloy	13
Figure 3.1	Task workflow	14
Figure 3.2	Technical Drawing Sample – Cylindrical Tool Pin	19
Figure 3.3	Temperature Profile of Heat Treatment Process	21
Figure 3.4	Fabrication of FSW via CNC Milling Machine	22
Figure 3.5	METASERV 2000 Grinder/ Polisher Machine	24
Figure 3.6	Electrochemical corrosion unit setup at Center for Corrosion Research (CCR)	25
Figure 4.1	Tunnel Defect on AA1100	29
Figure 4.2	Crack propagated along AA7075 during FSW process	30
Figure 4.3	Mapping Analysis on AA6061 with 0.1M NaCl Immersion Test	36
Figure 4.4	Tafel Plot Justification	39
Figure 4.5	Comparison on Tafel Plot for Base alloy and Weld Region AA6061	38
Figure 4.6	Tafel Extrapolation for base alloy (top) weld region AA6061	41
Appendix 2	FSW Tool – Square pin Technical Drawing	50
Appendix 3	FSW Tool – Cylindrical pin Technical Drawing	50
Appendix 4	FSW Tool – Tapered pin Technical Drawing	50
Figure 5.1	CNC Lathe Machine for Tool Fabrication	53
Figure 5.2	Carbolite Tube Furnace for heat treatment purposes	53
Figure 5.3	Fabrication of Mounting for Potentiostatic Experiment purposes	54
Figure 5.4	ACM measurement equipment	54

LIST OF TABLES

No	Table Name	Page
Table 2.1	Corrosion prone region in FSW of aluminum alloys	11
Table 3.1	FYP1 and FYP2 Gantt Chart	16
Table 3.2	Nominal Composition of Aluminum Alloy AA6061	17
Table 3.3	Nominal Composition of Aluminum Alloy AA1100	17
Table 3.4	Chemical Composition of AISI H13 Tool Steel	18
Table 3.5	FSW Process Parameter	22
Table 3.6	Electrodes used in the Electrochemical cell Testing	26
Table 4.1	FSW Aftermath Process Result	28
Table 4.2	Comparison before and after various tool design condition	31
Table 4.3	Microstructure of Base Metal and weld region of AA1100 and AA6061 via Optical Microscope	32
Table 4.4	Characteristic of AA6061 microstructure via FESEM	34
Table 4.5	Characteristic of AA1100 microstructure via FESEM	35
Table 4.6	Low magnification optical micrograph illustration on AA6061 material	38
Table 4.7	Results of corrosion test of AA6061 in 3% NaCl Solution	42
Table 5.1	AISI H13 Tool Pin properties and Specification	49
Table 5.2	Data of Polarization Potentiostatic measurements via ACM Potentiostat	55

CHAPTER 1:

INTRODUCTION

1.1 BACKGROUND OF STUDY

Alloys have become one of the most widely range used materials in marine and aerospace industries because of their good mechanical properties, high strength, high toughness, better corrosion resistance and recycling capabilities ^{[10][20]}. AA6061 is one of the most used in the 6000 series alloy, especially in the usage of transportation components, machinery equipments, recreational products and consumer durables. The highlight of the AA6061 usage in this project is about the common usage of this material in marine frames and various pipelines ^[21]. Basically, this type of aluminum alloy contains magnesium and silicon as its major alloying components (see Table 3.2 and 3.3 for nominal composition of Aluminum Alloy AA1100 and AA6061) ^[22]. These major compositions contribute to the higher strength of the material via precipitation hardening ^[23].

There are a lot of methods in the welding process; in our subject of interest is a solid state type welding. The context of solid state welding is that it does not involve the melting of the materials being joined. The energy from the impact plasticizes the materials, forming a weld, even though only a limited amount of heat is generated. ^[1] Friction Stir Welding (FSW) Process is one type in these categories alongside ultrasonic welding, explosion welding, cold welding and electromagnetic pulse welding.

In the end, the joint is achieved when localized heating from the rotating tool and translation leads to movement of material from the combination of the front/back of the pin softens the material around the pin ^[2].

1.2 PROBLEM STATEMENT

1.2.1 Problem identification

There have been reports that the Tungsten Inert Gas (TIG) and Metal Inert Gas (MIG) welding processes will conclude changes to the corrosion properties of the AA6061 and cracking often occurs without filler metals ^[5]. As example of metal inert gas study, peak current and pulse frequency have direct proportional relationship with the pitting corrosion resistance of the welded joints (if the peak current is increased, the pitting corrosion resistance will be increased.) ^[24]

FSW have advantages compare to the metal inert gas welding because of solid state process. However, the effect is this process induces dramatic changes in microstructures. The high corrosion resistance of Al alloys are largely depends on the heterogeneity of their microstructure ^[4]. Thus, there is every need to understand the microstructure and corrosion behavior of friction stir welds.

1.2.2 Significant of the project

The recent demand for Autonomous Underwater Vehicles (AUV) requires smaller and energy-efficient technology for marine propeller. One of the major areas that are being intensely highlighted is the selection of suitable material. Marine propellers are usually made from metal-based material such as manganese–aluminum–bronze and nickel–aluminum–bronze ^[19].

Composite propellers cannot be repaired and difficult to produce in small sizes. Stainless steel is extremely durable and allows blades to be as thin as possible to reduce resistance in the water. Stainless steel propellers are also stronger and allow for modifications or repair work. However, it is quite expensive. The most versatile material is aluminum alloy propellers which is lightweight than stainless steel, have high corrosion resistance and fortunately, they meet the required part for marine application. In addition, aluminum blades can also be repaired ^[19].

Therefore, this study can aid and facilitate the information of FSW process impact on the AA6061 corrosion properties. The study also provides sufficient supply data and any informational facts in the study of Friction Stir Welding. Furthermore, this medium can be used to close up the gap towards the knowledge in deeper aspect of corrosion study.

1.3 OBJECTIVE

The present investigation is aimed at the study of microstructure and corrosion resistance of AA 6061 and AA1100 Aluminum alloy that been welded by the mean of Friction Stir Welding process. AA1100 was be used as reference material as the composition of AA1100 is similar to the unalloyed aluminum.

1.4 SCOPE OF STUDY

This case study will be on the research of the corrosion resistance and centers to the two types of Aluminium Alloy; AA1100 and AA6061 and the effect of the differences in the tool pin that affected the corrosion properties. We have determined to use a familiar type of tool pin which is an American Iron and Steel Institute (AISI) H13 Tool Steel Grade. The process of planning and designing the tool pin were conduct by utilizing CATIA V5 R14, and further fabricate our Tool Steel with Computer Integrated Machine (CIM) CNC Lathe Machine. Due to the high temperature involvement projected by our tool, AISI H13 Tool Steel will undergo heat treatment process with specified temperatures to increase its hardness level. After FSW process using CIM CNC Milling Machine, the material were observed to study the corrosion properties of the particular material.

These microstructures suggested to be characterized by the mean of optical microscopy (OM) and Field Emission Scanning Electron Microscopy (FESEM). The location of intergranular attack relative to the welding nugget following the exposure to ASTM G-34 modified solution can be illustrated by low magnification optical micrograph ^[25]. The observation on the corrosion current (I_{corr}) properties suggested

to be studied in 3% NaCl solution at a constant temperature of 30°C (room temperature).

1.5 THE RELEVANCY OF PROJECT

Friction Stir Welding Process has the potential of avoiding significant changes in its properties as it being a solid process. However, previous studies shows that temperatures during FSW are sufficiently high, and the times were long it influence strengthening precipitate morphologies ^[4]. Thus, in the end of the joining process, there exist a post-weld gradient in the precipitate distribution from the parent metal to the weld nugget region. This study will give clear information in the affect of corrosion properties along different region.

1.6 FEASIBILTY OF THE PROJECT

This project was conducted in two semesters of total eight (8) months. First semester were more of literature review and concept understanding in FSW. The fabrication of the tool pin and its heat treatment also conducted in the first term of the project. In second semester, fabrications of FSW process have been done at Block N-4. The experiment was conducted at Block 17 (sample preparation and optical microscopy), Block P (FESEM) and the Electrochemical Corrosion Testing were completed at Centre for Corrosion Research, Block I Academic Complex. All experiment was conducted within Universiti Teknologi Petronas.

CHAPTER 2: THEORY AND LITERATURE REVIEW

2.1 The Ideas of Friction Stir Welding (FSW)

Recently, aluminum alloy have been used widely for automotive, shipbuilding and aircraft products, railway rolling stock industries and most likely others. The frequent usage of aluminum in variety of field is largely due to the fact that aluminum are light in weight compared to other material, easy to machine and have relatively high tensile strength.

However, aluminum alloys such that 6061 are difficult to join by conventional fusion welding machines ^[4]. Hence realizing a fusion-welded joint in such alloys without impairing the mechanical properties is a difficult task for the welding engineer. Consequently the welding engineer has to rely on rivets and fasteners with substantial increase in fabrication cost and structure weight. In products of fusion welding processes such as Tungsten Inert Gas (TIG) and Metal Inert Gas (MIG), hot cracking often occurs without filler metals ^[5]. These problems can be eliminated by Friction Stir Welding process ^[6].

Unlike other bulk thermomechanical (TM) welding processing operations, the highly localized nature of FSW introduces steep thermal and deformation gradients into the material adjacent to and along the joint line ^[7]. Therefore, standards and specifications for friction stir technologies must of necessity address and account for the localized metal working nature of friction stir technologies.

Friction Stir welding is essentially a hot working process where a large amount of deformation is induced into the work piece through pin and shoulder and the temperature never exceeds 0.8 TM (TM is the melting point of the material) ^[8]. The first attempt at classifying microstructures was made by P.L. Threadgill ^[9]. This was further revised and accepted by the friction stir welding association.

2.1 The Process of Friction Stir Welding (FSW)

FSW use the fundamental of using non-consumable rotating tool with its design and configurations been established associated with the material properties. A schematic of the weld process is shown in figure 2.1. In order to friction stir weld a butt or lap joint, a specially designed cylindrical tool is rotated and plunged into the joint line.

The tool has a small diameter pin with a concentric larger diameter shoulder. When descended to the part, the rotating pin contacts the surface, at the same time heats the material because of rapid friction, and softens a small column of metal. As the pin penetrates beneath the surface, part of this metal column is extruded above the surface. The tool shoulder and length of entry probe control the depth of penetration ^[10].

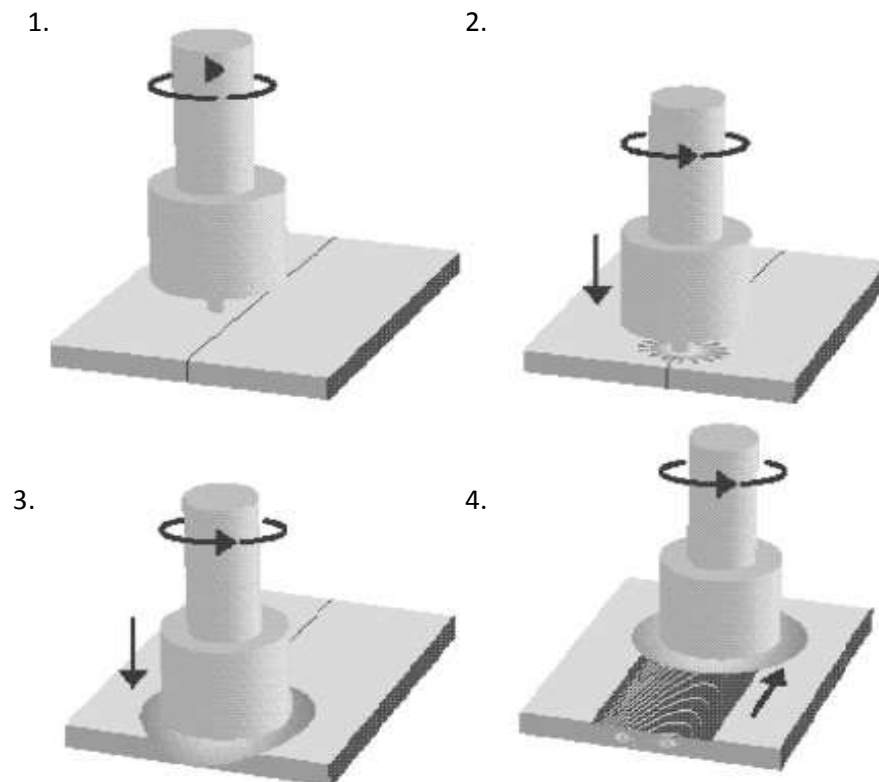


FIGURE 2.1: Schematic of the Friction Stir Welding Process

From Figure 2.1:

1. The start of the process requires the tool pin to rotate at the adequate rotation and spindle speed. In the picture shows the rotating tool prior to penetration into the butt joint of the material.
2. The tool pin begins to make contact with the aluminium alloy. This contact will eventually create additional heat and help to plasticize a larger cylindrical metal column around the inserted pin.
3. As the tool goes further, the shoulder starts to make contact with material. As the two surfaces make contact, it restricts further penetration while expanding the hot zone. The shoulder also provides a forging force that contains the upward metal flow caused by the tool pin.
4. This is further followed by the movement of each other such that the tool tracks the weld interface. The rotating tool provides continual heat working action, plasticizing metal within a narrow zone, while transporting metal from the leading face of the pin to its trailing edge.

From figure 2.2 below, we can see the outcome of the Friction Stir Welding process. The moving column of stirred material hot metal consumes the weld interface, disrupting and dispersing aluminium surface oxides. The weld cools, not solidifies, as the tool passes, forming a defect-free weld outcome. These weld process will generates some types of zones unique to FSW which will be discussed later.

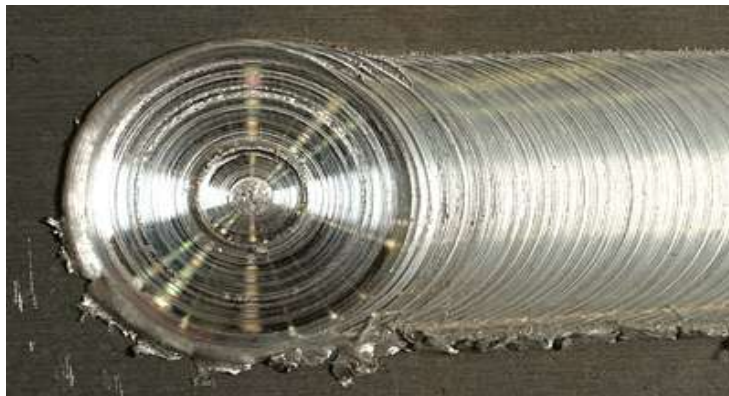


FIGURE 2.2: FSW Process Material Ending Product

2.3 Friction Stir Welding Microstructural Zones

^[11] As mentioned before, FSW process consists of 4 main types of microstructural zones due to the aftermath of the process which are:

- a) Unaffected material/ parent metal/ base metal
- b) Heat affected zone (HAZ)
- c) Thermo – mechanically affected zone (TMAZ)
- d) Weld Nugget

Figure 2.3 below shows the position of each of the zones with respect to the material welded parts.

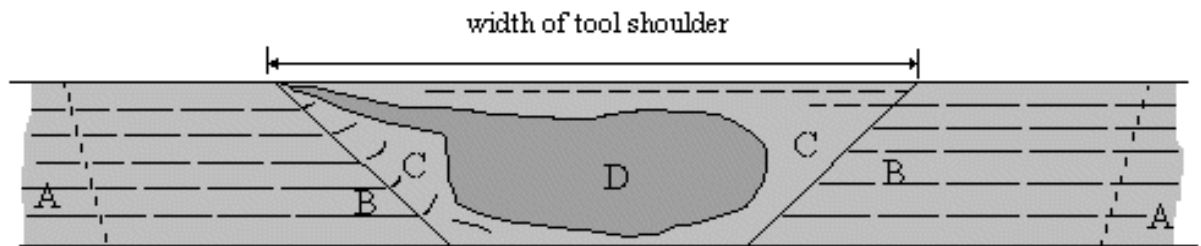


FIGURE 2.3: Cross sectional Area of the Material with respect to Microstructural Zones

A: Unaffected material/ Parent metal

Material remote from the weld, which has not been deformed and although it may have experienced a thermal cycle from the weld is not affected by the heat in terms of microstructure or mechanical properties.

B: Heat affected zone (HAZ)

The region which is lie closer to the weld centre compared to the parent metal. A Heat Affected Zones (HAZ), the metal experienced thermal transient and significant changes in temperature. In other hand, HAZ zones did not experience any plastic deformation.

C: Thermo – mechanically affected zone (TMAZ)

TMAZ consist of two regions. The main TMAZ zone is which zone adjacent to the weld nugget affected by heat (C region). This region has changes in temperature and plastic deformation, but it will not experience any recrystallization. The other one TMAZ is the weld nugget region.

D: Weld Nugget

Weld nugget were the fully recrystallized, fine grain region in the weld center, surrounded by TMAZ region. The microstructure of weld nugget by rubbing the rear face of the shoulder, and the material may have cooled below its maximum.

There are also terms associated with FSW to describe the regions surrounding the weld or processed region which are advancing side and the retreating side. Figure 2.4 below shows the idea of the terms.

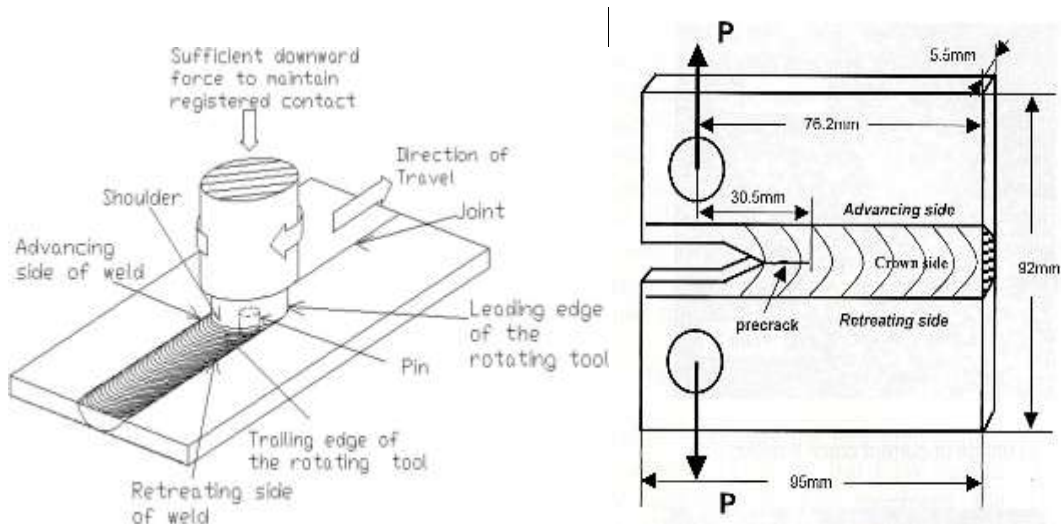


FIGURE 2.4: Advancing and Retreating Side of FSW

Advancing side of the FSW process is the side of the weld which the tool rotation and the travel direction are in the same direction. In the other hand, retreating side is the opposite of advancing side as the side of the weld is in the reversing direction from the travel route [12].

2.4 FSW Tool Design

Tool design for Friction Stir Welding (FSW) consists of several designs that can be considered to be the concept for further evaluation. This tool design is one of the important parameters which influence heat generation, plastic flow, the power required and the uniformity of the welded joint^[13]. Figure 2.5 below shows the basic parts contained in the FSW tools.

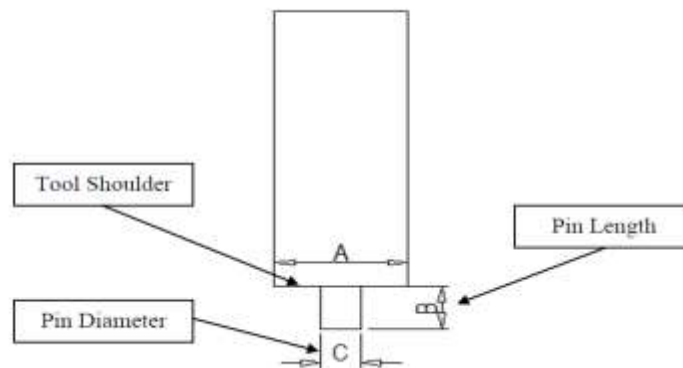


FIGURE 2.5: FSW tool basic dimensions

- A. Pin Length** – The length necessarily reviewed to avoid significant contact with the anvil.
- B. Pin Radius** – Radius should be sufficient for adequate pin strength and also for stretching the seam, to expose tolerable clean surface for a good bond
- C. Tool Shoulder** – Shoulder must wide enough so that it can avoid the metal from escaped

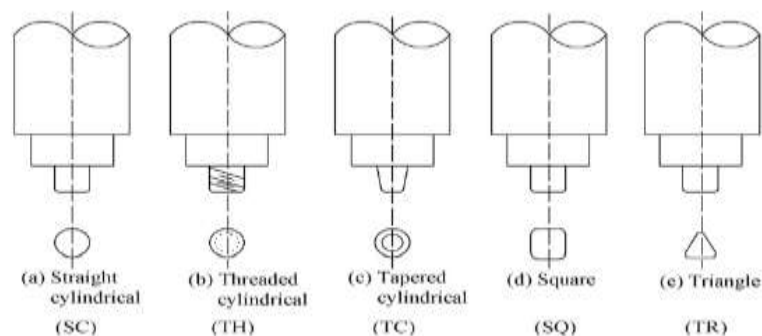


FIGURE 2.6: Key design of the FSW Tool Pin Profiles.

2.5 Corrosion Perception View

The microstructure resulted by friction stir process in precipitation hardenable aluminum alloys are different from that of base metal microstructure or cast structure of fusion welds. These changes can bring a difference in corrosion properties of the weldment.

Generally, a passive oxide film can be readily formed on the surface of aluminum alloys, when exposed to air or water. However the corrosion rate could be very high due to the presence of chloride ions ^[9]. Furthermore, the corrosion behavior of aluminum alloy is largely due to the heterogeneity of their microstructures. As the friction stir process induces a dramatic change in microstructures, there is every need to understand the microstructure and corrosion behavior of friction stir welds.

Table 2.2 lists the most susceptible regions for corrosion resistance for corrosion in friction stir welds of different aluminum alloys, identified in various earlier studies ^[14].

Base material	Corrosion-prone region
AA2024	TMAZ
	None _a
AA2024	SZ
	HAZ
	SZ and HAZ
AA2195	None _a
	TMAZ
AA5454	None _a
AA5083	None _a
AA5456	SZ
AA7010	SZ
	HAZ
AA7050	SZ/TMAZ boundary
AA7150	TMAZ

*a - Weld corrosion resistance comparable or superior to base material.

Table 2.1: Corrosion-prone regions in friction stir welds of various aluminum alloys ^[14]

2.6 Corrosion Mechanisms

Aluminium alloys are widely used in structures where a high strength to weight ratio is important, such as in the marine frames applicatio. Aluminium has a natural corrosion protection from its oxide layer, but if exposed to aggressive environments it may corrode. Still, if correctly fabricated, constructions of aluminium may be reliable and have long service life ^[26].

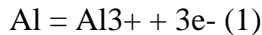
2.6.1 Oxide Destabilization

The following factors may affect the stability of the aluminium oxide and thereby cause corrosion:

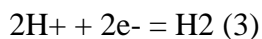
- The oxide is not stable in acidic (pH < 4) or alkaline (pH > 9) environments.
- Aggressive ions (chlorides, fluorides) may attack the oxide locally.
- Certain elements (Ga, Tl, In, Sn, Pb) may become incorporated in the oxide and destabilise it ^[27].

2.6.2 Pitting

Pitting is a highly localized type of corrosion in the presence of aggressive chloride ions. Pits are initiated at weak sites in the oxide by chloride attack. Pits propagate according to the reactions



while hydrogen evolution and oxygen reduction are the important reduction processes at the intermetallic cathodes, as sketched in figure 1:



As a pit propagates, the environment inside the pit (anode) changes. According to reaction 2 the pH will decrease. To balance the positive charge produced by reaction 1 and 2, chloride ions will migrate into the pit. The resulting HCl formation inside

the pit causes accelerated pit propagation. The reduction reaction will cause local alkalinisation around cathodic particles. As previously mentioned aluminium oxide is not stable in such environment, and aluminium around the particles will dissolve (alkaline pits). The active aluminium component of the particles will also dissolve selectively, thereby enriching the particle surface with Fe and increasing its cathodic activity. Etching of the aluminium matrix around the particles may detach the particles from the surface, which may repassivate the alkaline pits. This may also reduce the driving force for the acidic pits causing repassivation of some in the long run.

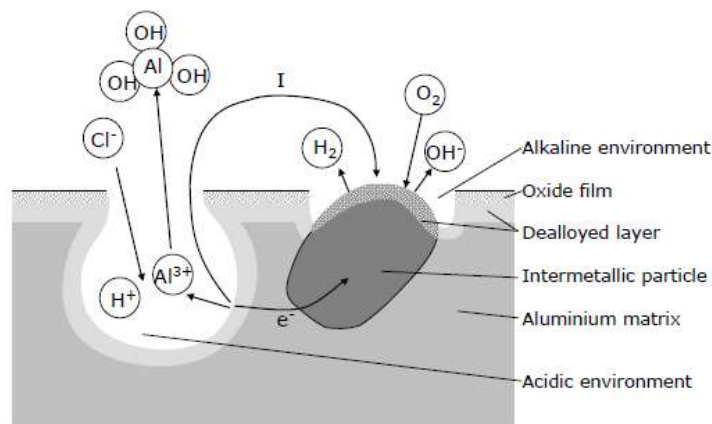


FIGURE 2.7: Generalised illustration of pitting corrosion on aluminium alloys

2.6.3 Intergranular Corrosion Attack

Intergranular corrosion (IGC) is the selective dissolution of the grain boundary zone, while the bulk grain is not attacked ^[28]. IGC is also caused by microgalvanic cell action at the grain boundaries. The susceptibility to IGC is known to depend on the alloy composition and thermomechanical processing. Grain boundaries are sites for precipitation and segregation, which makes them physically and chemically different from the matrix. Precipitation of e.g. noble particles at grain boundaries depletes the adjacent zone of these elements, and the depleted zone becomes electrochemically active. The opposite case is also possible; precipitation of active particles at grain boundaries would make the adjacent zone noble.

CHAPTER 3: METHODOLOGY

3.1 Task Workflow

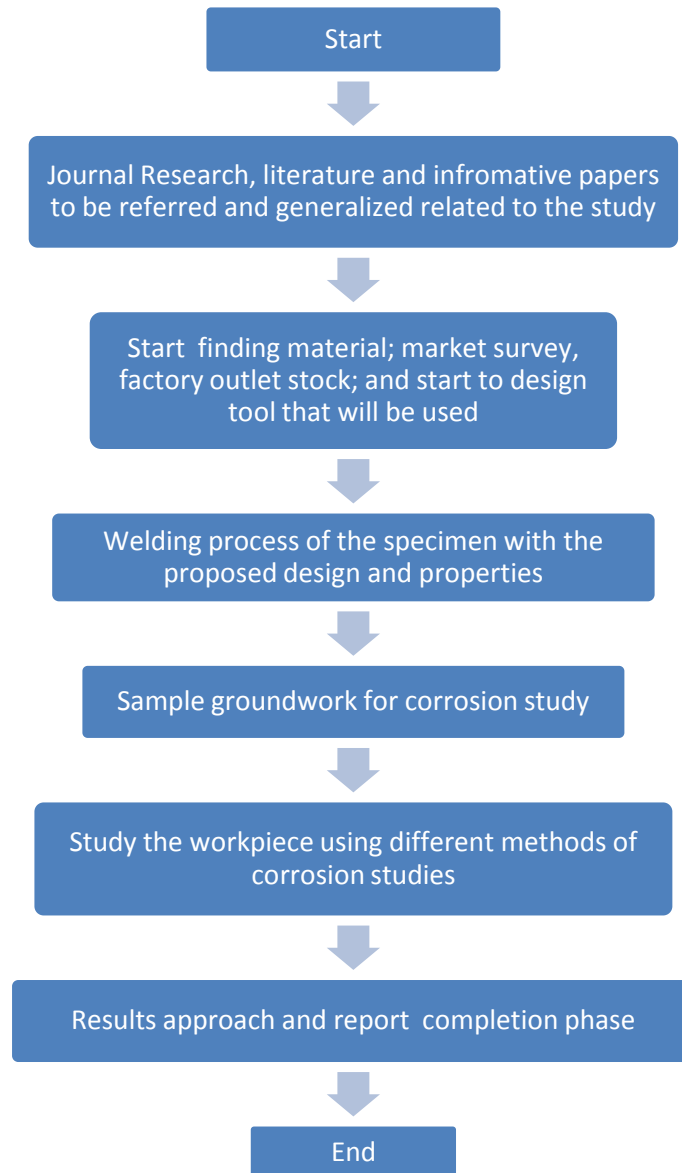


Figure 3.1: Task workflow for the entire study

3.2 Project Milestones and Gantt chart

Here are listed the prospect that would be needed to completed in Final Year Project I:

1. Material and Tools finding and study the sustainability of each other
2. Fabricate needed tool pin to pursue for FSW process
3. Heat treatment process for all of the tool pin
4. Sample preparation for the upcoming Fabrication of the work piece by the means of Friction Stir Welding Processing in the future

The key milestones that will be completed for Final Year Project (FYP2) are listed as:

1. Completion of Friction Stir Welding (FSW) using desired tool pin for a specific butt jointed type.
2. Preparation of the specimen related to the further corrosion behavior study
3. Start on investigation of the corrosion properties of friction stir welded joint result using plenty of methods.
4. Results been taken, discussed, further deep research and finally finishing up the final report.

Final Year Project 1 (FYP1) and FYP2 Gantt Chart

No	Detail/ Week	1	2	3	4	5	6	7	Mid Semester Break	8	9	10	11	12	13	14	
1	Project topic selection phase	█															
2	Review of common studies in FSW Concept	█	█	█													
3	Literature review – concept research of material and tooling of FSW			█	█	█	█	█			█	█	█	█	█	█	█
4	Proposal and Proposal Defense completion										█	█					
5	Selection of the desired material and tool pin for upcoming research											█	█				
6	Fabrication and heat treatment of desired tool pin													█	█	█	█
7	Sample preparation for FSW process and interim report submission																█

No	Detail/ Week	1	2	3	4	5	6	7	Mid Semester Break	8	9	10	11	12	13	14	
1	Maintaining the study of literature review	█	█	█	█	█	█	█			█	█	█	█	█	█	█
2	Friction Stir Welding Process			█	█	█	█										
3	Preparation of the material for the experiment							█			█	█					
4	Equipment preparation for the experiment											█					
5	Execute experiment with respect to corrosion research											█	█	█			
6	Results compiled and researches been done													█	█	█	█
7	Final report														█	█	

Table 3.1: FYP1 (above) and FYP2 (below) Gantt Chart

3.3 Material Selection for Specimen and FSW Tool

Some of the listing and elimination process been done to decide the best material and tool that will be used for the upcoming experiment. In the material point of view, we need to pick two (2) different materials to rectify a comparison between it. The decision of picking up AA1100 Aluminum alloy is because it is a base metal of aluminum, basically 99.5% minimum of it is contained by aluminum.

Tool pin selection have been done by referring to the melting point of both material that been used. In that case, we have decided to take AISI H13 Tool steel. This is by the fact that the H13 tool steel is categorized as hot work tool steel (Type H). It can function well at elevated temperatures by combining good hardness and abrasion resistance to resist heat cracking up to 600 – 1000°F^[15].

Table 3.2 and 3.3 below shows the nominal composition of both AA6061 and AA1100 aluminum alloy whereas in Table 3.4 shows the chemical composition of AISI H13 Tool Steel.

	Zn	Mg	Cu	Cr	Al
Weight %	0.25	1.2	0.4	0.35	Rest

Table 3.2: Nominal Composition of AA6061 Aluminum Alloy

	Zn	Mg	Cu	Mn	Al
Weight %	0.01	-	0.05	0.05	99.5 min

Table 3.3: Nominal Composition of AA1100 Aluminum Alloy

Element	Weight %
Carbon (C)	0.40
Manganese (Mn)	0.35
Silicone (Si)	1.05
Chromium (Cr)	5.00
Molybdenum (Mo)	1.30
Vanadium (V)	1.00

Table 3.4: Chemical Composition of AISI H13 Tool Steel

The AA1100 will be put side by side with AA6061 type of aluminum alloy to investigate the effect of different composition with the related corrosion resistance. AA6061 is been used because it is one of the most high strength aluminum alloy compared to its other companion in the same kind. High strength precipitation hardening of 6xxx series aluminum alloys, such as 6061 is used extensively in aerospace.

3.4 Fabrication of the FSW Tool

This experiment requires the fabrication of different tool pin to give much more influences to the result of the upcoming experiment. There were three (3) types of tool pin (refer Appendices) which is cylindrical, tapered and square shape pin. Both design of Cylindrical and Tapered were fabricated by using Computer Numerical Control (CNC) Lathe Machine BridgePort PowerPath 15. The square shape pin fabricated by using CNC Machine MAZAK.

Figure 3.2 and below shows the examples of the technical drawing for the tool pin.

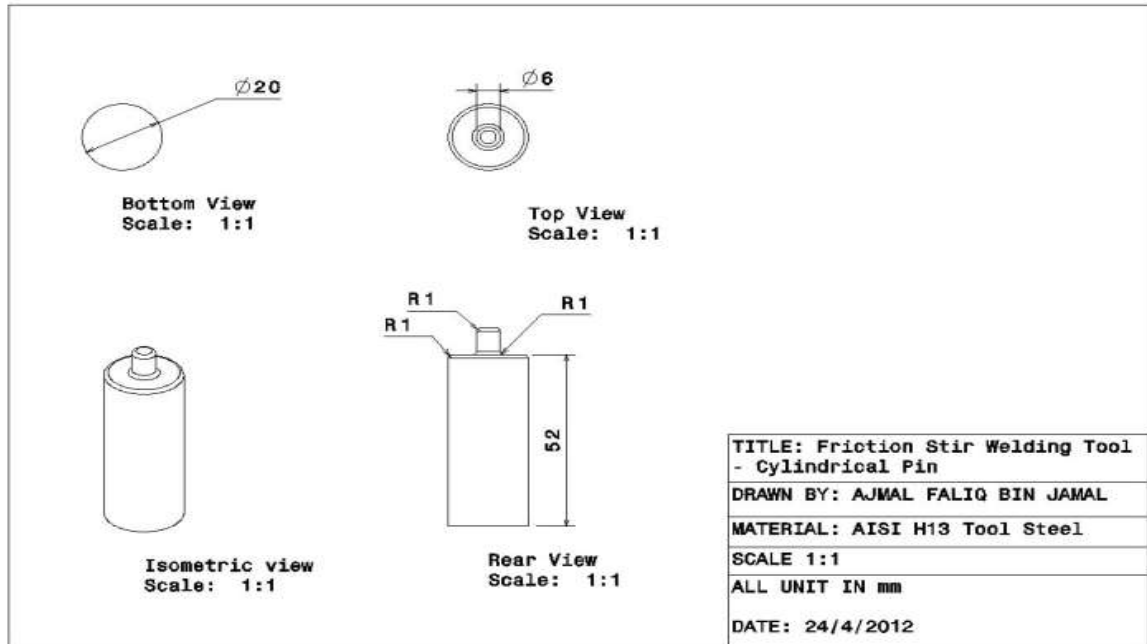


Figure 3.2: Technical Drawing Sample – Cylindrical tool pin

From the drawing shown, the required dimensions for the fabrication of the tool were specified. Besides the basic dimensions, which are pin diameter, pin length and tool shoulder diameter, the design also contain the entire fillet used in the respected edges. The drawings were completed using CATIA Software Version V5R14.

Both machines used to fabricate have its delicate requirements that need to be emphasized. As such, for CNC Machine – MAZAK used to fabricate square pin, the minimum dimension for the material necessitate is a 35mm in diameter and 95mm length. The design of square tool pin have different tool pin length (5mm) compare to the square and tapered design (8mm) due to the constraint of the MAZAK machine used to fabricate the square tool design profile.

3.5 Heat Treatment of AISI H13 FSW Tool

Heat treatment is a group of industrial and metal working processes used to alter the physical, and sometimes chemical, properties of a material (source: Wikipedia). Heat treatment for Friction Stir Welding (FSW) is very important because the process deals with very high amount of heat that can cause damages to either material or the tools. ^[16] From this fact, a tool with heat treating process has the upper hand because of the following criteria:

1. Heat treated metal can restore ductility after a cold working operation
2. Improves both the formability and machining ability of the tool
3. Increase the strength of the material
4. Improve the overall product performance by certain desirable characteristics

For this experimental purpose, we have use the heat treatment furnace that is readily available for student use in UTP. The model of the furnace is Carbolite Heat Treatment Tube Furnace located at Mechanical Building Block 17. ^[16] The procedures of suitable heat treatment are determined by studying the basic properties of AISI H13 Tool Steel.

Procedures below shows the heat treatment that been undergo by the material and **Figure 3.3** shows the plotting of the temperature Vs time.

Heat Treatment Procedure, AISI H13 Tool Steel:

1. The entire welding tools designs are inserted into the Tube Furnace. The machine initially preheat the tool for to (2) hours to rise up the temperature from 30°C to 732°C.

2. The process preceded by continuous heating from 732°C to 760°C slowly for another two (2) hours.
3. Next, the temperature rose up to 1000°C for one (1) more hour.
4. Finally, it is cooled back down to its initial temperature of 30°C for last two (2) hours.

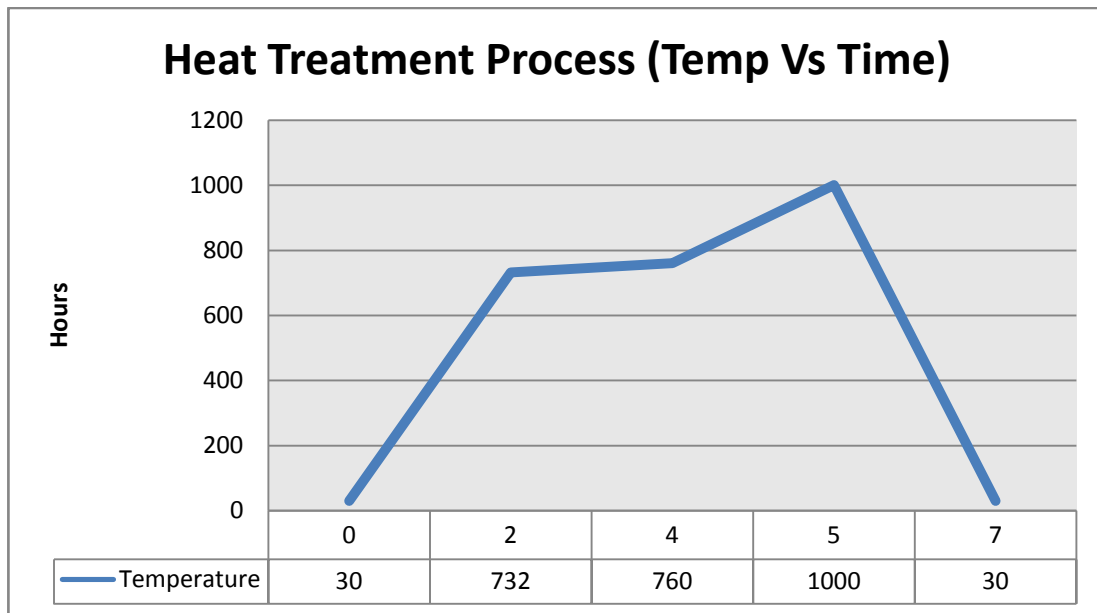


Figure 3.3: Temperature profile of the Heat Treatment Process

3.6 Friction Stir Welding (FSW) Process

For the purpose of preparation, we have to ensure all important point, such as the process parameter and the material set up would be determined to ease our flow in finishing the process.

As the tool pin is fabricated by CNC Lathe Machine Bridge Port, the FSW process will use CNC Milling Bridge Port VMC 2216 at block N. Several parameters that is needed in the process such as:

1. Horizontal feed rate (mm/ min)
2. Spindle speed (rpm)
3. Plunging feed rate (mm/ min)
4. Penetration (mm)

Dwell time is an ample time to generate high temperature towards bottom of the weld. **Table 3.5** is the suggested parameters that were used for the experiment with the advice from supervisor and respective technician.



Figure 3.4: Fabrication of Friction Stir Welding via CNC Milling Machine

FSW Tool Pin Profile	Traverse Feed Rate, (mm/ min)	Spindle Speed (rpm)	Plunging Feed Rate (mm/ min)	Penetration, (mm)	Dwell time, s
Cylindrical Pin	15	1600	10	-8.1	20
Tapered Pin	15	1600	10	-8.1	20
Square Pin	15	1600	10	-5.1	20

Table 3.5: FSW Process Parameter

3.7 Sample Preparation for Microstructure Scanning

The study of microstructure of physical structure, configuration and component were generally called as metallography. In the process of preparation for the scan process, the surface of the sample is prepared by various methods of grinding, polishing and etching^[18]. As this preparation was subjective, the style of planning the process can be a choice of technique. Nonetheless, these modus operandi were beneficial in identifying alloys and predicting any particular material properties related to the specimen.

3.7.1 Specimen Sizing and Standard

Prior on the progress in microstructural study that will be seen after the corrosion submergence, it is required that the samples would be cut into appropriate dimension that can give detailed explanation for the results. The hacksaw machine, located in Block 21 Academic Complex, UTP is suitable for the process. Besides, the specimen that will be submerged into chemical substance should be fitted in the compartment.

3.7.2 Grinding and Polishing

The purpose of grinding in the first place would be to eliminate any marks and levels, also to unsoil the surface of the specimen. Polishing in the other hand removes the damages and spot of grinding. This can be accomplished with steps of successively finer abrasive particles. The test was carried out at Block 17 Lab, Academic Complex UTP using METASERV 2000 Grinder and Polisher Machine (**Figure 3.5**). Grinding material used is an abrasive paper covered with silicon carbide grits. The stages of the grinding process is primarily depended from the coarse to the finer type abrasive paper ranging from 180, 240 up to 1200, the highest quality finish suitable for the material. Rotational speed of the machine is set to be 200 rpm and water been used as the lubricant. In addition, grinding process introduce only limited amount of new deformation.



Figure 3.5: METASERV 2000 Grinder/ Polisher Machine for grinding and polishing process

3.7.3 Etching

The final step for microstructure preparation is etching. Etching is a process that been performed in order to enhance the features of the microstructure of the specimen in optical manner to determine the phase attribution and grain size. In addition, etching process would change the microstructure features based on composition that is visible with the usage of the microscope. Chemical etching involves the immersion process of the specimen in particular chemical solution. This will be done in a period of time before the final rinsing for sanitary purposes. The Keller's reagent used in this etching process contains 5ml of nitric acid, 3ml of hydrochloric acid (HCl) and 2ml of hydrofluoric acid and finalized by distilled water (190ml).

3.8 Sample Preparation for Corrosion Tests

3.8.1 *Electrochemical Cell*

In order of obtaining the corrosion rates of the sample, polarization resistance testing would be an option. The tests been done by taking the current readings of the cell during a short and slow sweep of the potential. For standard purposes, the sweep was taken from (-100 to +100) mV relative to Open Circuit Potential (OCP) ^{[5][8]}. The tests performed by using ACM Potentiostat (**Figure 3.6**) supported by corrosion measurement software (Version 5) equipped with the ACM setup.



Figure 3.6: Electrochemical corrosion unit setup at Center for Corrosion Research (CCR)

Scan rate defines the speed of the potential sweep in the range of mV/sec. These are helpful for the purpose of getting the results because of almost linearly curve between current density and voltage curve. The estimation of the polarization resistance is given by the linear data fitting of the specimen, which then used for calculation of the corrosion current density (I_{corr}) and corrosion rate.

3.8.2 *Sample Preparation for Corrosion*

In this study, there are three (3) electrodes that should be integrated to undergo the testing. The electrodes which involved in electrochemical cell would be working electrode (WE), reference electrode (RE) and auxiliary electrode (AE). **Table 3.6** below shows the respected electrodes with the samples and materials used.

Electrode	Material/ Specimen
Working Electrode (WE)	FSW Samples
Reference Electrode (RE)	Silver/ Silver Chloride (Ag/ AgCl)
Auxiliary Electrode (AE)	Stainless Steel Electrode

Table 3.6: Electrodes used in the electrochemical cell testing

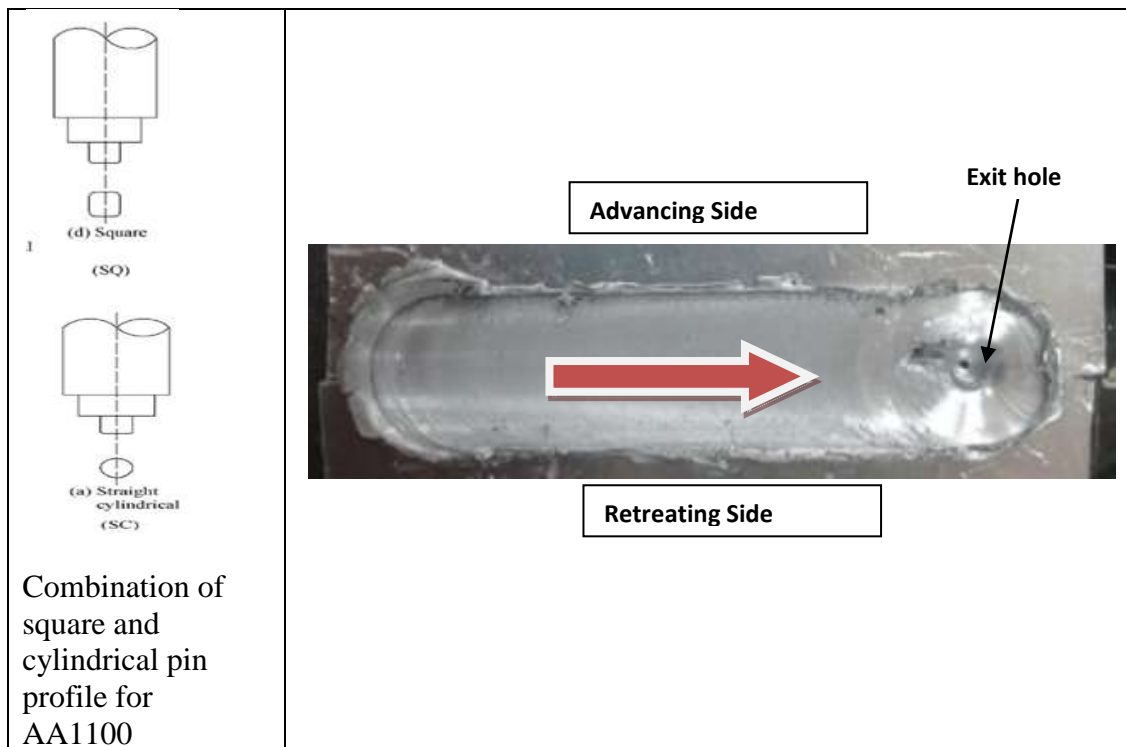
In addition to the electrodes arrangement, there are additional areas that also need to be implemented. The samples would be fitted to the container and mounted by resin and hardener. The ratio of resin and hardener were 5:1. 1cm² plate of the weld joint (contain both thermo – mechanically affected (TMAZ) and heat affected (HAZ)), and also the base metal should be prepared. After that, these samples would be exposed to 3% sodium chloride (NaCl) solution. The potentiodynamic scan will be undergone with the setting of 10mV/min scan rate.

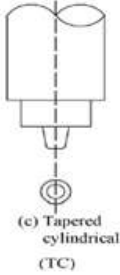
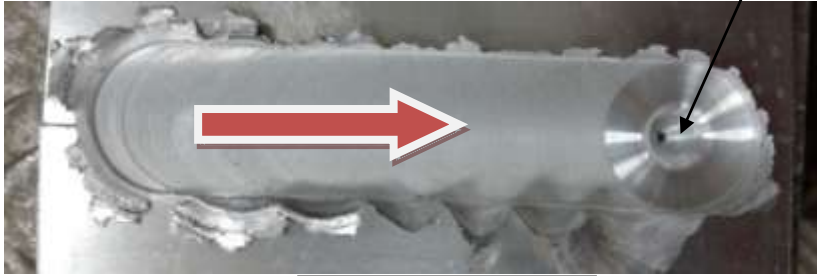
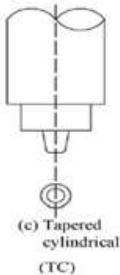
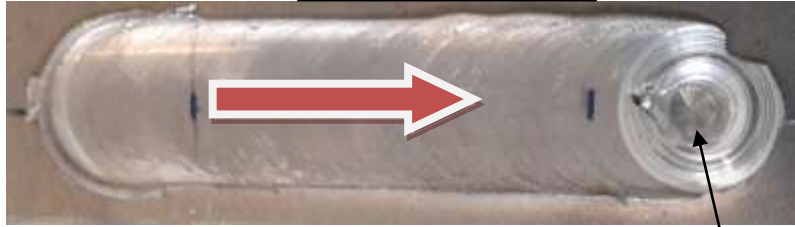
Prior to the potentiostatic polarization experiment, job safety analysis (JSA) and procedure have been prepared for the lab usage at CCR. (Refer Appendices)

CHAPTER 4: RESULT AND DISCUSSION

4.1 Friction Stir Welding Result

In the start of Final Year Project 2 (FYP2) duration, the progress of the project continued with the proceedings of the friction stir welding process. In the first half of the timeline, the Aluminium Alloy AA1100 is to be completed first, using square + cylindrical tool combination and tapered shaped tool. Noted that the square shaped tool have been weld twice because the tip of the square shaped have been limited to 5mm (refer to **Table 4.1**). As the result, the square shaped undergo a backup FSW using the cylindrical design.



 <p>(c) Tapered cylindrical (TC)</p> <p>Tapered shaped tool pin for AA1100</p>	
 <p>(c) Tapered cylindrical (TC)</p> <p>Tapered shaped tool pin for AA6061</p>	

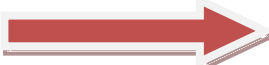
Note:  Direction of travel

Table 4.2: Friction Stir Welding Aftermath Process Result

4.2 Defects on the FSW Aftermath Process

The result of the overall process shows several obvious defects in the weld zone particularly. This imperfection would probably due to the fact that the material of AA1100 receive inadequate amount of heat during the welding process ^[17]. As confirmed in the Figure 4.2, the observation shows the result of the AA1100 using square and cylindrical tool pin profile have visible defect on the surface of the aftermath welding.

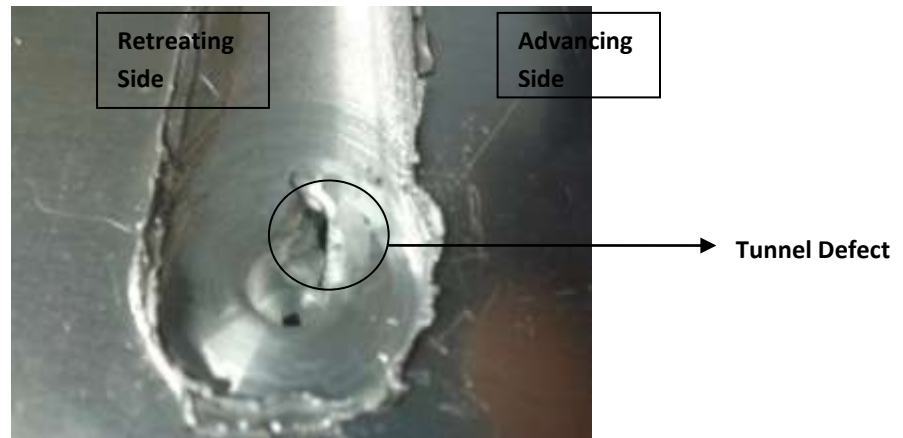


Figure 4.1: Tunnel defect on AA1100; Square and Cylindrical Tool Pin

As related to this defect, there are also other side effects such as porosity, solidification or slag inclusion that can react during the fusion welding and would compromise the quality of the outcome results. Although there might be chances, the process can be concluded as a success because of minimal effects that the process has occurred. This can be related for the reason that there is no melting stages during FSW and the material are joined in the solid state itself due to heat generated by the friction from tool and plate, causing the flow of metal by stirring action.

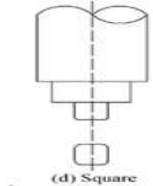
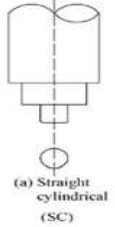
After finishing the FSW process of AA1100, we have determined to proceed with the second material. At first place, the desired material that is planning to be used was AA7075. Unluckily, the FSW operation was interrupted with some irregular deformation of the material (figure 4.2). The slip-up would maybe because of the improper parameters that been used and the limited coverage of tools used. In the end, we decided to proceed with AA6061 which also commonly used in aerospace and marine industry, same with the case of AA7075 but still in the scope of study and precise objectives.



Figure 4.2: Crack propagated along AA7075 during FSW process

4.3 Effect on Tool Pin Profile

The completion of the Friction Stir Welding process also affecting the physical appearances and the shapes compare to the origin shapes. **Table 4.3** compares the before and after the process.

Tool Pin Profile	Condition: Before Process	Condition: After Process
 <p data-bbox="396 1304 483 1335">Square</p>		
 <p data-bbox="370 1625 516 1656">Cylindrical</p>		

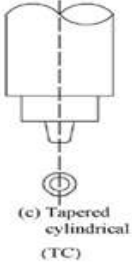
 <p>(c) Tapered cylindrical (TC)</p> <p>Tapered</p>		
--	---	---

Table 4.2: Comparison before and after of the various tool design condition

As referring to the previous table, the most apparent changes of the visible appearances would be the square shaped tool pin profile. Other shapes, which resemble the shape of the tool rotation (circular), did have little transformation compare to square shape. We can foresee that the result is based on the fact that the circular friction of the tool pin that act upon the butt joint of the material and thus, causes deformation to the basis square shape of the tool.

4.4 Microstructure Examinations on different conditions

As friction stir welding is a solid state type of weldment, the joints are almost free from any defects. In other hand, fusion welding will result in several problems such as solidification cracks, slag inclusion and porosity which in return will jeopardize the base quality of the product ^[29].

Both of AA1100 and AA6061 were analyzed at low magnification (10x – 50x) using optical microscope to reveal and compare the quality of the weldment in different region. The figure shows (A) weld nugget region, and (B) base alloy of the material.

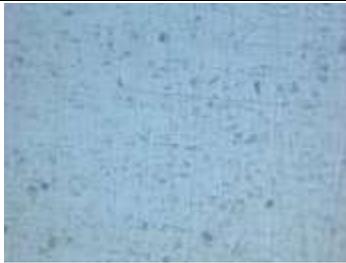
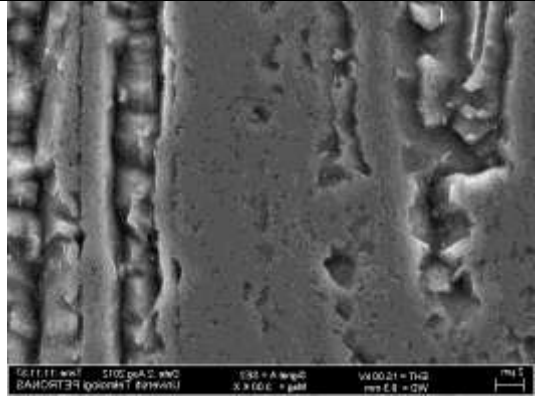
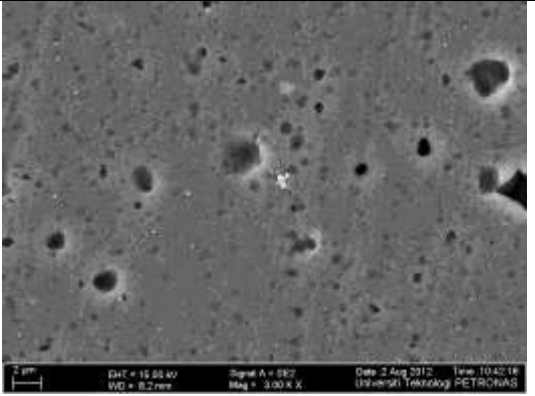
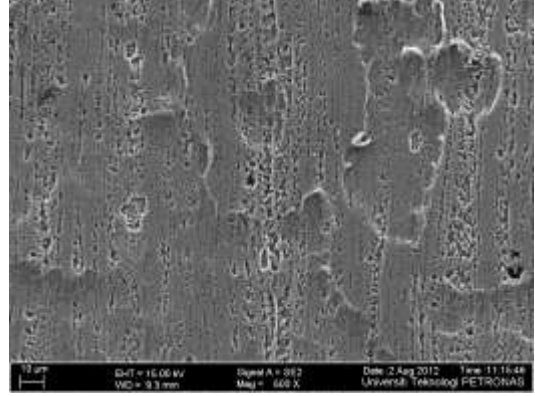
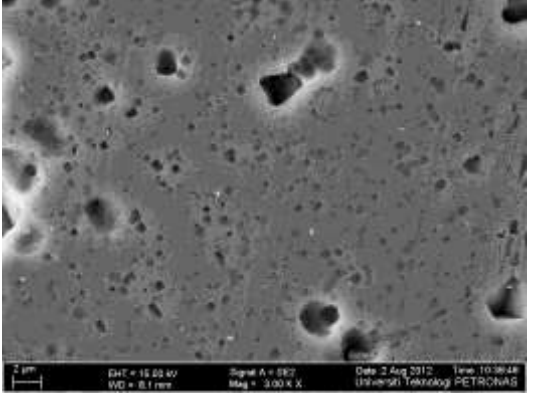
	Base Alloy Region	Weld Region (include HAZ and TMAZ)
AA1100 via Square + Cylindrical Tool Pin		
AA1100 Tapered Tool Pin		
AA6061 Tapered Tool Pin		

Table 4.3: Microstructure of Base metal and Weld Region for AA1100 and AA6061 via Optical Microscope (50x Magnification)

From the observation of the results, it is concluded that the joint have different profile on the occasion of different region. Base metal has finer microstructure compared to the weld region. This result also indicates that fine particles homogeneously distributed in the base alloy. Note that grain boundaries are not distinguishable in the base alloy using this imaging mode.

4.5 Microstructure and Pitting Observation via Field Emission Scanning Electron Microscope (FESEM)

FESEM observations and analysis were conducted using Carl Zeiss AG SUPRA 55VP located at Block P, Academic Complex UTP. The FESEM was used to study the second phase precipitates and the visualization on creation of pitting prior to the immersion on 0.1M NaCl solution. **Table 4.4 and 4.5** below shows the characteristic of Aluminum Alloy microstructure by means of FESEM.

	AA6061 with 0.1M NaCl Immersion	AA6061 without 0.1M NaCl Immersion
Weld Region		
Thermo Mechanical Affected Zone (TMAZ)		

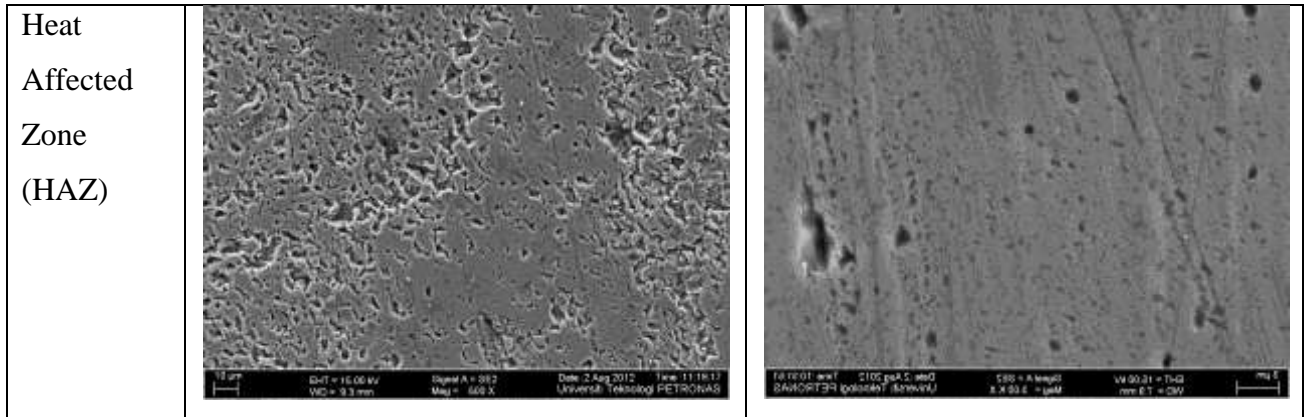


Table 4.4: characteristic of AA6061 microstructure by means of FESEM

Based on table above, the corrosion can be determined to localize mainly in the nugget region. The predominant pitting creation is also existed on nugget region. This is the evidence of cathodic reactivity found in the form of grooves around constituent intermetallic particles. The grooves around constituent particles are the consequence of the cathodic reduction of oxygen, which takes place at the constituent particles and causes an increase in alkalinity in the solution around the particles leading to the dissolution of aluminum matrix. **Figure 4.3** below maps the existence of oxygen in the immersed (0.1M NaCl) AA6061 material.

The microstructure of AA1100 (**Table 4.5** below) via FESEM has much clearer observation in the existence of pits. The results are the same; in fact, the localization on weld region is more coarse and there is obvious differences of the attack in this region compare to HAZ and TMAZ region.

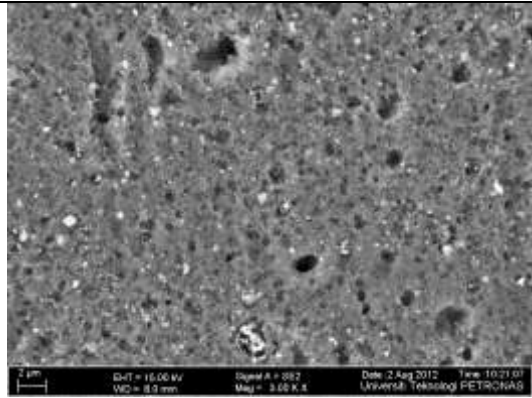
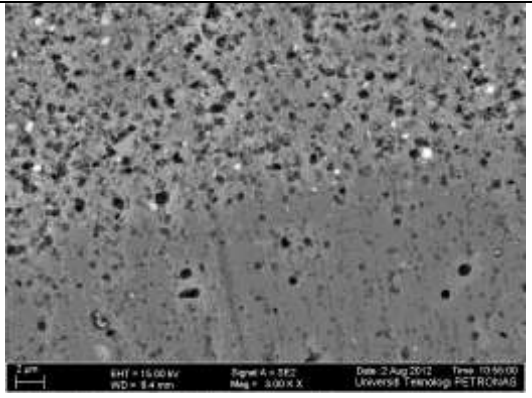
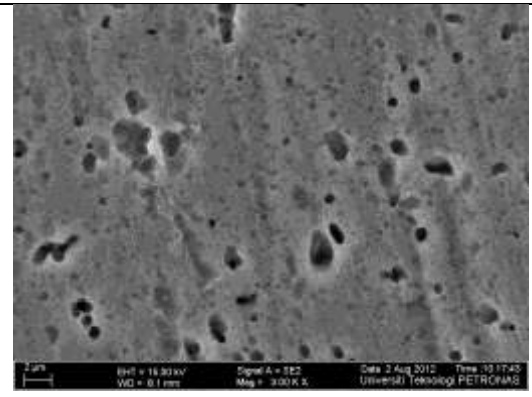
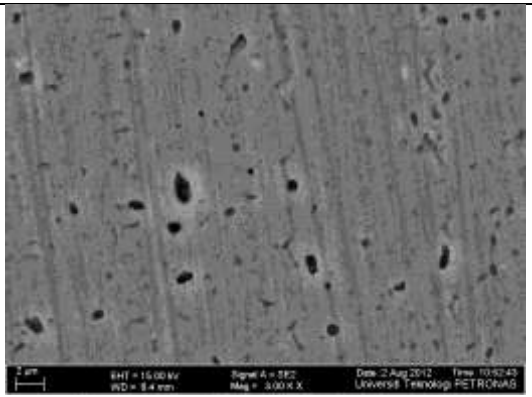
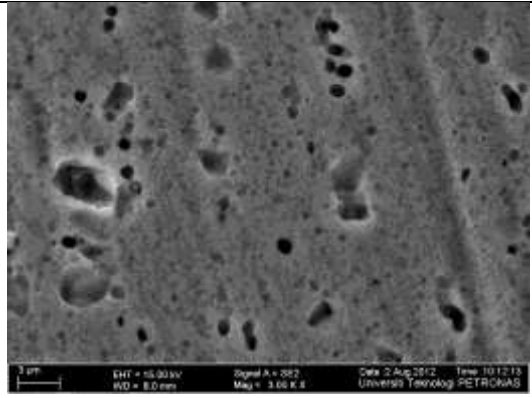
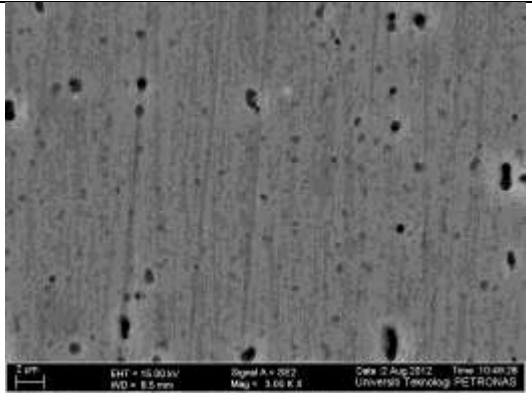
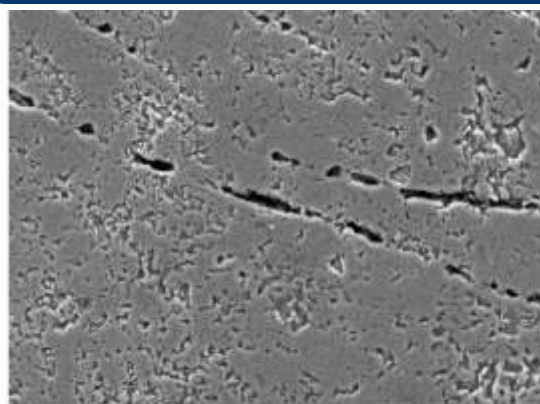
	AA1100 with 0.1M NaCl Immersion	AA1100 without 0.1M NaCl Immersion
Weld Region		
Thermo Mechanical Affected Zone (TMAZ)		
Heat Affected Zone (HAZ)		

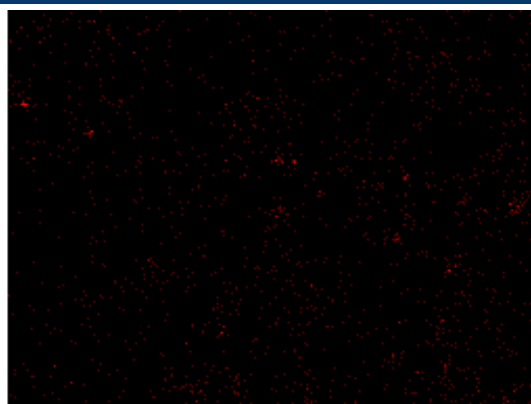
Table 4.5: characteristic of AA1100 microstructure by means of FESEM

4.6 Mapping Analysis Via FESEM of AA6061 prior to Immersion to 0.1M NaCl Solution

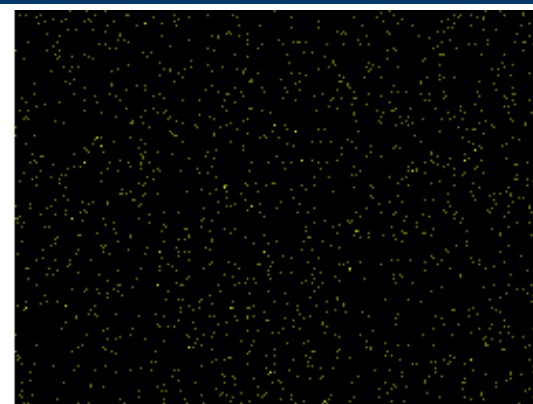
02/08/2012 11:48:12



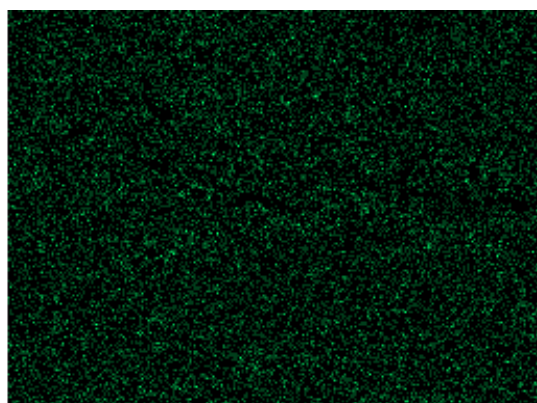
Electron Image 1



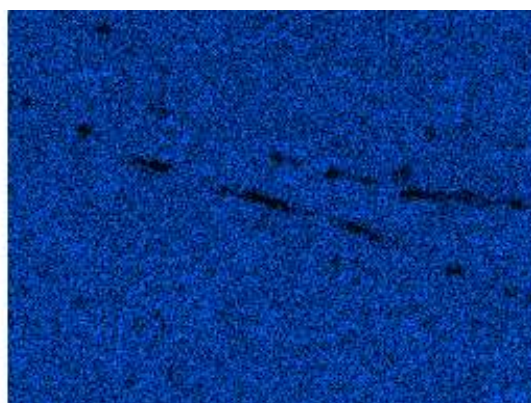
C Ka1_2



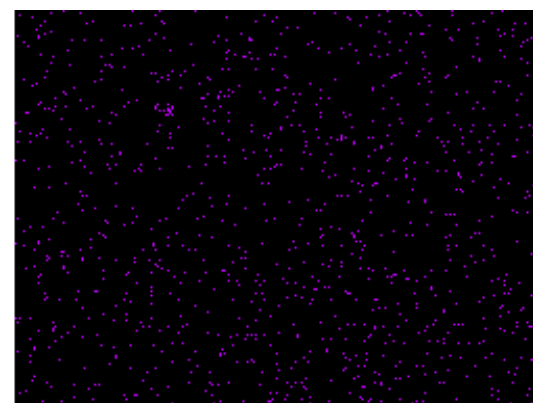
O Ka1



Mg Ka1_2



Al Ka1



Mn Ka1

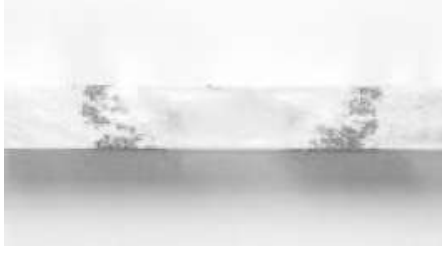
Figure 4.5: Mapping Analysis on AA6061 with 0.1M NaCl Immersion Test



4.7 Susceptibility to Intergranular Attack Study

Susceptibility to localized corrosion was evaluated using American Society for Testing and Material (ASTM) EXCO test (G-34). Accordingly, for the study performed, the specified test solution of 4M sodium chloride (NaCl), 0.5M potassium nitrate (KNO₃) and 0.1M HNO₃ was diluted to distinguish between different rates of corrosion attack for the different weld region microstructural conditions. The measured pH of the diluted EXCO solution was 1.90. Except where noted, test samples were exposed to these corrosive solutions for 24 h.

The results is not consistent with the immersion tests, but still in the scope of differentiating between the weld region with the base alloy. **Table 4.6** below shows the low magnification optical micrograph illustration on the AA6061 material.

Corrosion Solution 10% Dilution of ASTM G34 4M NaCl 0.5M KNO ₃ 0.1M HNO ₃	Low Magnification Optical Micrograph	Remarks
Day 2		No visual attack on base metal and nugget region, only initiation of intergranular attack in the HAZ region.
Day 4		For extended exposure times to the modified EXCO solution, the intergranular attack became more severe in the initial attack region. After ~ 72 h, evidence of intergranular attack also became more apparent in the HAZ and included all regions of the previously unattacked TMAZ.

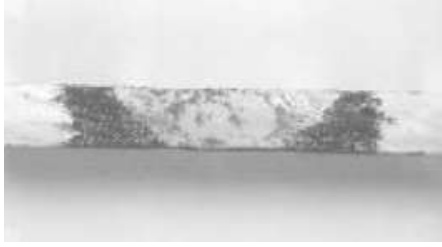
Day 7		For all observations, the corrosion attack in the weld region was intergranular, whereas no intergranular corrosion was detected in the parent metal.
-------	---	---

Table 4.6: low magnification optical micrograph illustration on the AA6061 material

From the table above, the most susceptible attack of the intergranular is at the HAZ region, where nugget region have been detected only after more than 120 hours. After the period of about 4 days, in the TMAZ region, the attack was distributed unevenly, even after 120 h, indicating an inhomogeneous microstructure and/or an inhomogeneous precipitate morphology following FSW deformation. In the end, there is no intergranular corrosion been identify at the base alloy indicating high corrosion resistance of AA6061. Although the result is not similar to the microstructure study (weld nugget have higher pitting existence), the scope of study are still in progress as the extent of the study was to oversee the whole corrosion properties changes resulting by the Friction Stir Welding process.

The conclusion that can be made in this experiment is that the friction stir welding process has jeopardized the corrosion properties of the material. All of the weld region (include weld nugget, TMAZ and HAZ) have sudden intergranular attack compare to the base alloy.

4.8 Potentiostatic Polarization Measurement via Tafel Extrapolation

In previous study, there have been several reports indicating a passive oxide film that is readily formed on the surface of aluminum alloys, when exposed to air or water. However the corrosion rate could be very high due to the presence of chloride ions. With an increase in the concentration of Cl^- , the pitting corrosion becomes severe and statistical maximum corrosion depth is consistent with Gumbel distribution. Furthermore, the scale of AA6061 usage lengthens to the marine application, which is in chloride environment.

In this study, electrochemical corrosion test by Tafel extrapolation method was carried out on all samples of base alloy weld region of AA6061 in sodium chloride solution of 3% NaCl to determine corrosion parameters, such as corrosion potential (E_{corr}) and corrosion current (I_{corr}) as shown in **Table 4.7**. **Figure 4.4** below justify the Tafel plotting. The corrosion rates of the material will depend on the corrosion current (I_{corr}). The higher corrosion rates capability will be resulted by a lower I_{corr} value. The I_{corr} value of welded region and base metal of AA6061 are compared to see the differences of the current rates.

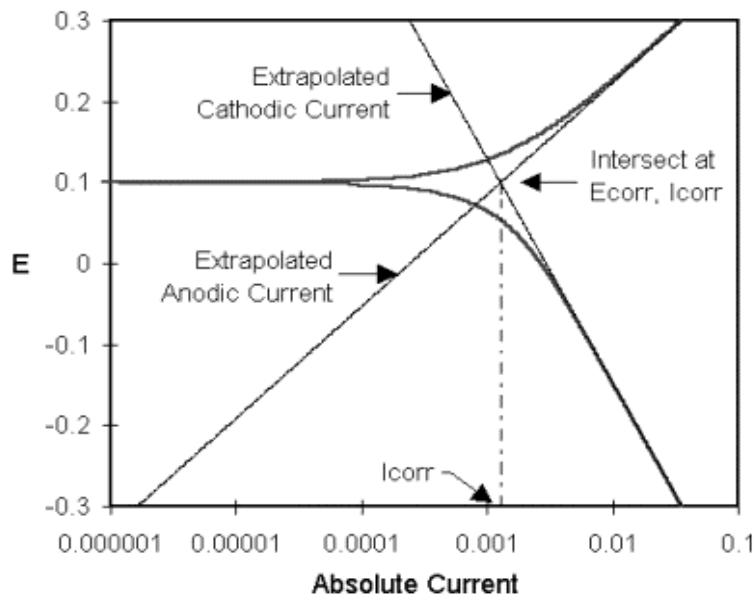


Figure 4.4: Tafel Plot Justification

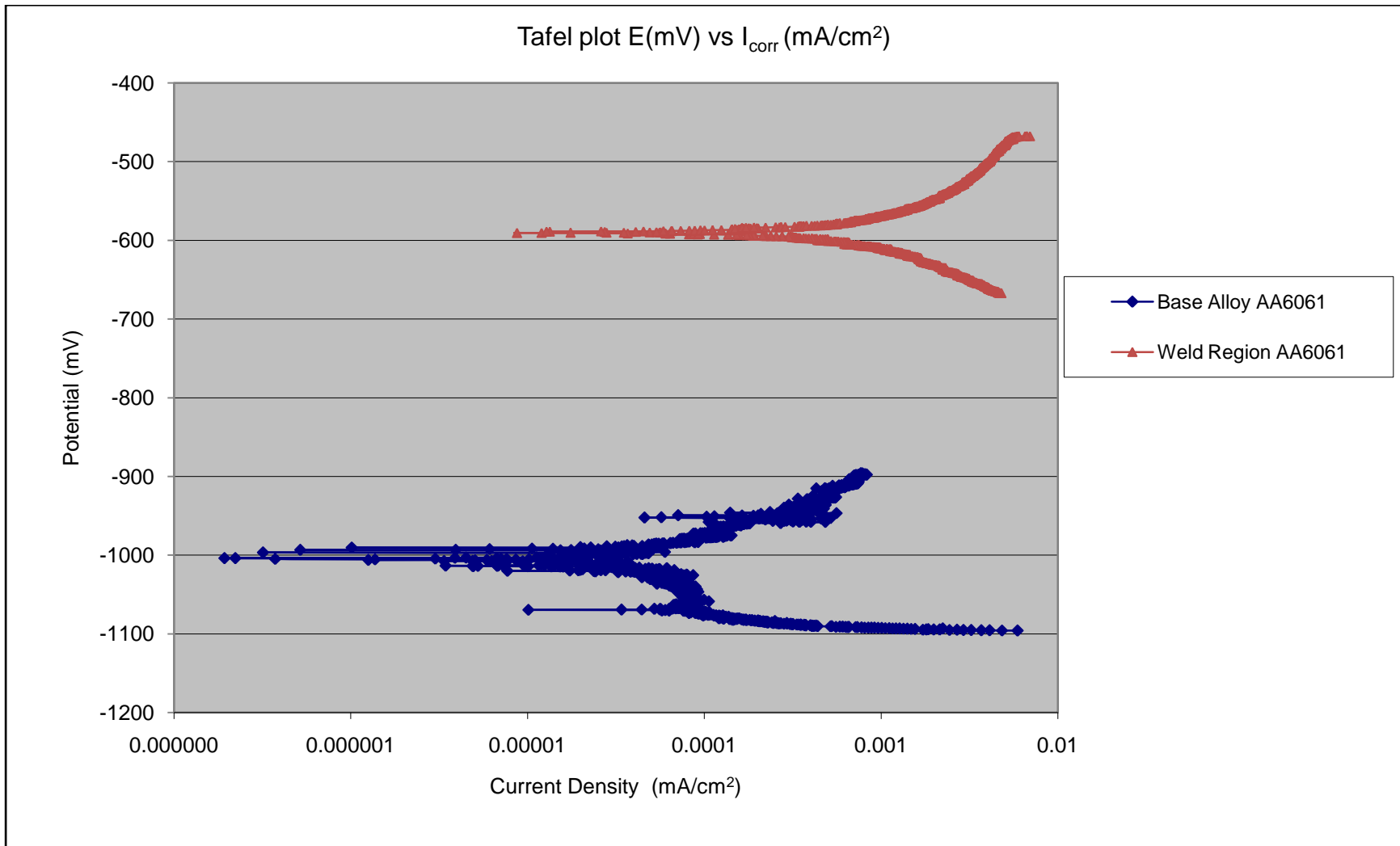


Figure 4.5: Comparison on the Tafel plot for base alloy and weld region of AA6061

Figure 4.5 shows the comparison of the two different graph with respect to the base and weld region. We can conclude that the base alloy have location indate the lower I_{corr} value and lower E_{corr} value compare to the weld region. **Figure 4.6** below were done to examine the value of E_{corr} and I_{corr} by means of Tafel extrapolation (done by using specialized corrosion measurement software) while **Table 4.7** were the results of the extrapolation.

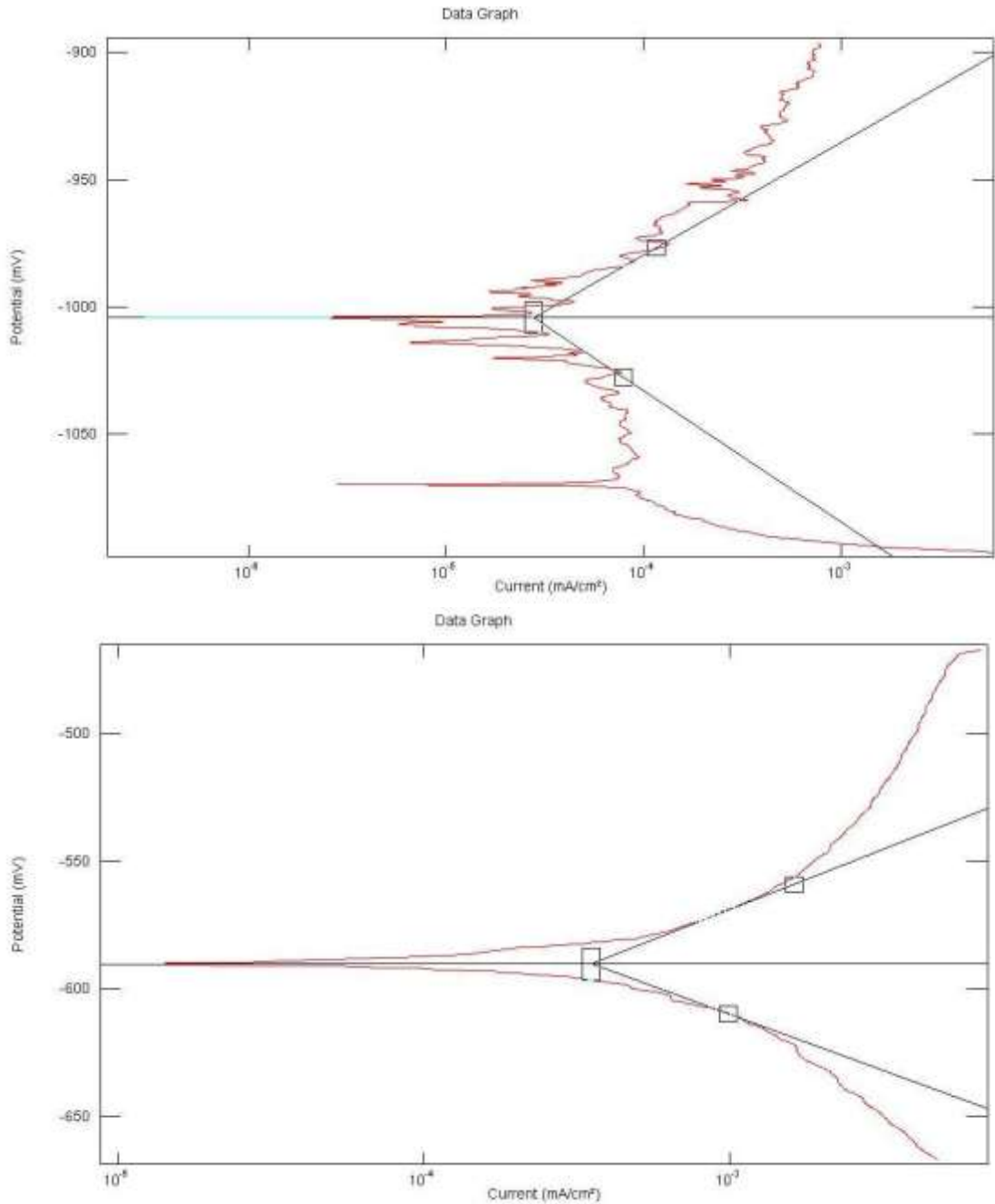


Figure 4.6: Tafel extrapolation for base alloy (top) and weld region AA6061

Sample	Ecorr (mV)	Icorr (mA/cm ²)	Corrosion Rates (mm/ yr)
Base Metal, AA6061	-1004	5.028E-05	5.592E-04
Weld Region, AA6061	-590.29	4.591E-04	5.1054E-03

Table 4.7: The results of corrosion tests of studied samples of aluminum alloy AA6061 in 3% NaCl solution

From the result above, it was shown that the corrosion behavior of base alloy significantly varies from that of welded joint, and the friction stir weld has higher corrosion current, Icorr (or less corrosion resistance) than base alloy. This is due to inhomogeneity of microstructure in weld regions or zones while the unwelded base alloy of AA6061 has a uniform microstructure i.e. uniform distribution of precipitates in aluminum matrix. The precipitates are nobler and promote anodic dissolution of the matrix.

From the value of Icorr, we can determine the corrosion rates by millimeter /year (mm/yr) with the equation:

$$\text{Corrosion Rate (mmpy)} = 0.00327 (\text{Icorr}) (\text{M/n}) /d$$

*where M/n (equivalent weight) of AA6061 = 9.813; density (d) = 2.7 g/cm³

The result of the corrosion rate were consistent with the Icorr; the base alloy have better corrosion rates (lower rates per year) compare to the weld region. However, as the result indicate that base alloy have better corrosion resistance to the weld region, the pitting potential E(mV) of weld region which is higher indicates better pitting resistance compared to base alloy; as opposed to the corrosion resistance results (Icorr).

CHAPTER 5:

CONCLUSION AND RECOMMENDATION

The initial process of finishing the friction stir welding (FSW) process have given better understanding of FSW itself, and the parameters with regards to the research on the tool pin material and design. The project was completed accordingly with respect to the plan and time frames that was designated before the start of the project.

The results prior to the several experiment completions prove that:

1. Following FSW of AA6061, weld zones were susceptible to intergranular attack. The hottest regions within the HAZ were the most susceptible to intergranular corrosion.
2. The weld nugget and deformed region of the TMAZ also were susceptible to intergranular corrosion, but to a lesser extent than the hottest region of the HAZ.
3. The mechanism of intergranular corrosion best correlated to a Cu depletion model linking intergranular corrosion with pitting corrosion.
4. Corrosion resistance of base aluminum alloy of AA6061 in 3%NaCl solution has been found better than that of friction stir weld
5. Corrosion potential (E_{corr}) of weld region is more noble (less negative) than that of weld joint (pitting corrosion resistance of weld metal is better than the base metal).
6. Corrosion rate of the base alloy are more superior to be compared to the weld region (weldment result leads to a decrease of corrosion rate (mm/yr) by almost 10 times worse).

From this project, it is recommended that:

1. As the FSW proved to jeopardize the corrosion properties of the AA6061, the usage of the FSW especially in marine environment (where high concentration of chloride solutions leads to high corrosion environment) should be monitored properly
2. Alternative of the process is cold forging (in terms of corrosion resistance, it is better because no involvement of high temperature). In the other hand, cold forging leads to less ductility. Intermediate anneals may be required to compensate for loss of ductility that accompanies strain hardening.
3. Corrosion protection of the Friction Stir Welds with conversion layer coatings is highly desirable.

REFERENCES

1. Stephan Kallee: *NZ Fabricators begin to use Friction Stir Welding to produce aluminium components and panels*, Paper published in New Zealand Engineering News, August 2006.
2. R.S. Mishra and Z.Y. Ma *Friction Stir Welding and Processing*, Material Science and Engineering R: Reports, 2005, Pages 1-78
3. Thomas, WM; Nicholas, ED; Needham, JC; Murch, MG; Temple-Smith, P; Dawes, CJ *Friction-stir butt welding*, GB Patent No. 9125978.8, International patent application No. PCT/GB92/02203, (1991)
4. Venugopal T, Rao KS, Rao KP *Studies on Friction Stir Welded AA 7075 Aluminum Alloy*, *Solid State Sciences*, Volume 11, Issue 4 (2004)
5. Muna KA, Hani AA, Khairia SH *Effect of Heat Treatment on Corrosion Resistance of Friction Stir Welded AA2024 Aluminum Alloy*, 1, (2011), 10.
6. Sutton MA, Yang B, Reynolds AP, Taylor R *Microstructural studies of friction stir welds in 2024 T3 aluminum*, 2, (2002) 7.
7. D. Burford, P. Gimenez Britos, E. Boldsai Khan, J. Brown *Evaluation of Friction Stir Weld Process and Properties for Aerospace Application: e-NDE for Friction Stir Processes*, National Institute for Aviation Research, Wichita State University, Wichita, KS FAA Joint Advanced Materials & Structures (JAMS) 6th Annual Technical Review Meeting (2010)
8. Muna KA, Basheer Ahmed AH, Sami AN *Study of Corrosion Behavior of Friction Stir Welded Aluminum Alloy (2024-T3)*, 1, 6.
9. Threadgill, TWI Bulletin (1997).
10. R Ahmad, MA Bakar *Effect of a Post weld heat treatment on the mechanical and microstructure properties of AA6061 joints welded by the gas metal arc welding cold metal transfer method*, *Materials and Design* 32 (2011) 5120 - 5126
11. *Microstructure Classification of Friction Stir Welds*, <http://www.twi.co.uk/content/qual>, (2011)

12. R Steel, Q Liu, M Collier, J Peterson, R Rowland, S Parker, MegaStir Technologies, *Friction Stir Welding: New Developments for Oil and Gas Industry*, 2010, Pages 1-7
13. AC Nunes, *Friction Stir Welding*, Innovation in Materials Manufacturing, 2011, pg 137 – 165.
14. Rao K., Janaki Ram GD, Stucker BE *Improvement in Corrosion Resistance of Friction Stir Welded Aluminum Alloys with Micro Arc Oxidation Coatings*, Scripta Materialia, Volume 58, Issue 11, June 2008, Pages 998-1001
15. CB Smith, JF Hinrichs, *Friction Stir Welding*, Innovation in Materials Manufacturing, 2011, pg 241 - 302.
16. AK Radzi, *Study on Worm Defect in Aluminium Alloy Friction Stir Welding Welded Plates*, Interim Report for Final Year Project, Universiti Teknologi Petronas, Malaysia (2011)
17. R Nandan, T Debroy and HKDH Bhadesia, *Recent Advances in Friction Stir Welding – Process, Weldment Structure and Properties*, University Of Cambridge, Cambridge, UK (2008)
18. ME 3701 Report, *Experiment: Metallography Specimen Preparation and Examination*, Materials of Engineering, LSU.
19. B. Abdullah, S. M. Sapuan, Z. Samad, H. M. T. Khaleed and N. A. Aziz ; *Manufacturing of AA6061 propeller for AUV application using cold forging process*; Scientific Research and Essays Vol. 7(2), pp. 170-176, 16 January, 2012
20. Missori S. Sili A. *Mechanical behavior of 6082 – T6 aluminum alloy welds*. J Metal Sci Technol 2000; 18 (1): 12-8
21. Elangovan K. Balasubramaniam V *Influences of post weld heat treatment on tensile properties of friction stir-welded AA6061 aluminium alloy joints* J Mater Char 2008; 59:1168–77.

22. Mrowka G, Sreniawski J. *Influence of heat treatment on the microstructure and mechanical properties of 6005 and 6082 aluminium alloys*. J Mater Process Technol 2005; 162:367–72.

23. Ozturk F, Sisman A, Toros S, Kilic S, Picu RC. *Influence of aging treatment on mechanical properties of 6061 aluminium alloy*. J Mater Des 2010; 31:972–5.

24. T.Senthil Kumar, V.Balasubramanian, M.Y.Sanavullah and S.Babu *Effect of Pulsed Current TIG Welding Parameters on Pitting Corrosion Behaviour of AA6061 Aluminium Alloy*, J. Mater. Sci. Technol., Vol.23 No.2, 2007 223 – 229

25. M. Jariyaboon, A.J. Davenport, R. Ambat, B.J. Connolly, S.W. Williams, D.A. Price *The effect of welding parameters on the corrosion behaviour of friction stir welded AA2024–T351*, Corrosion Science 49 (2007) 877–909

26. Gaute Svenningsen, *Corrosion of Aluminium Alloys*, Department of Materials Technology, 7491 Trondheim, Norway

27. Nisancioglu, K., *Corrosion of aluminium alloys (Proceedings of ICAA3)*, volume 3, pages 239-259. Trondheim, 1992. NTH and SINTEF.

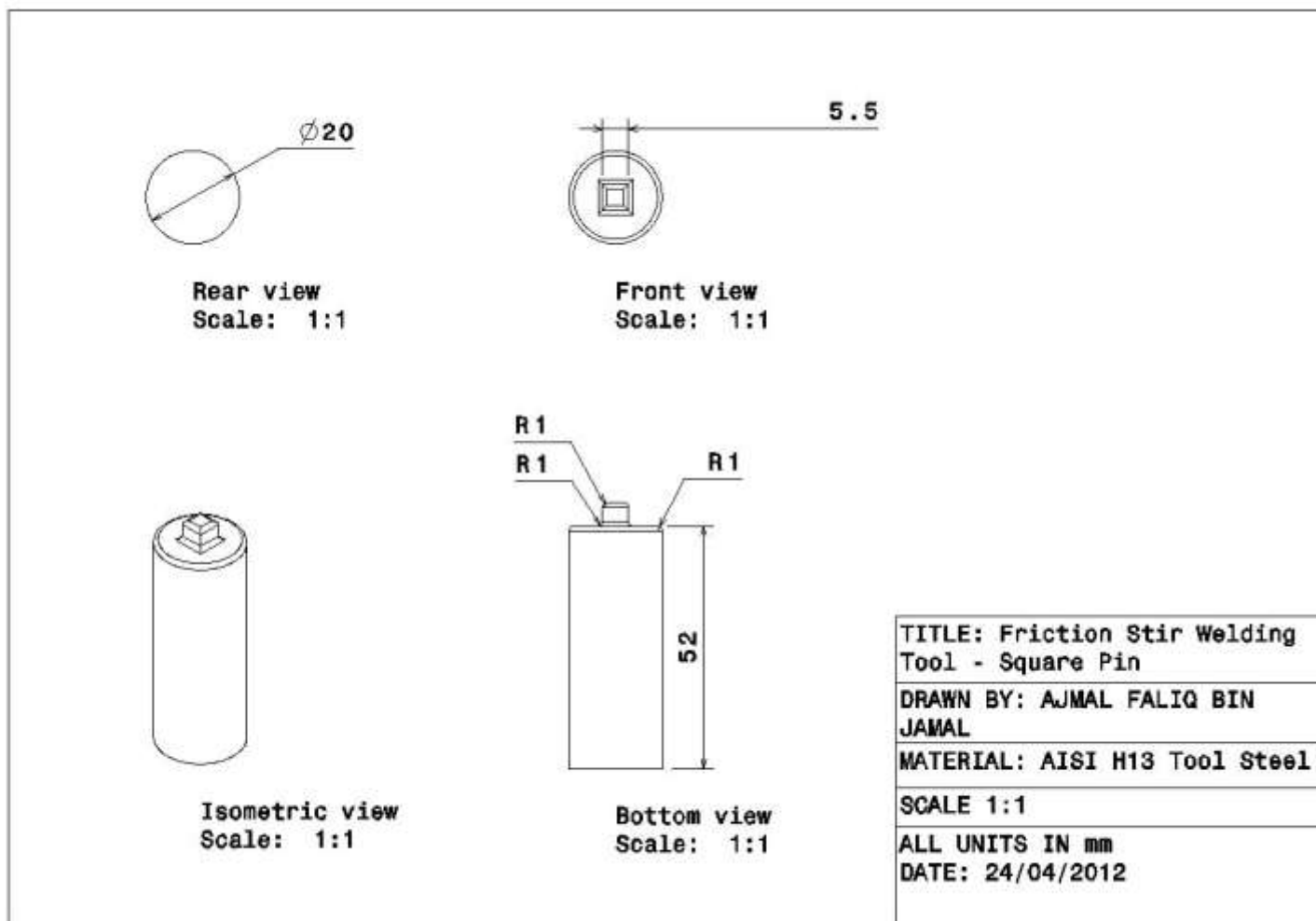
28. Hatch, J. E., editor. *Aluminium - Properties and physical metallurgy*, pages 242-264. ASM, Ohio, 1984.

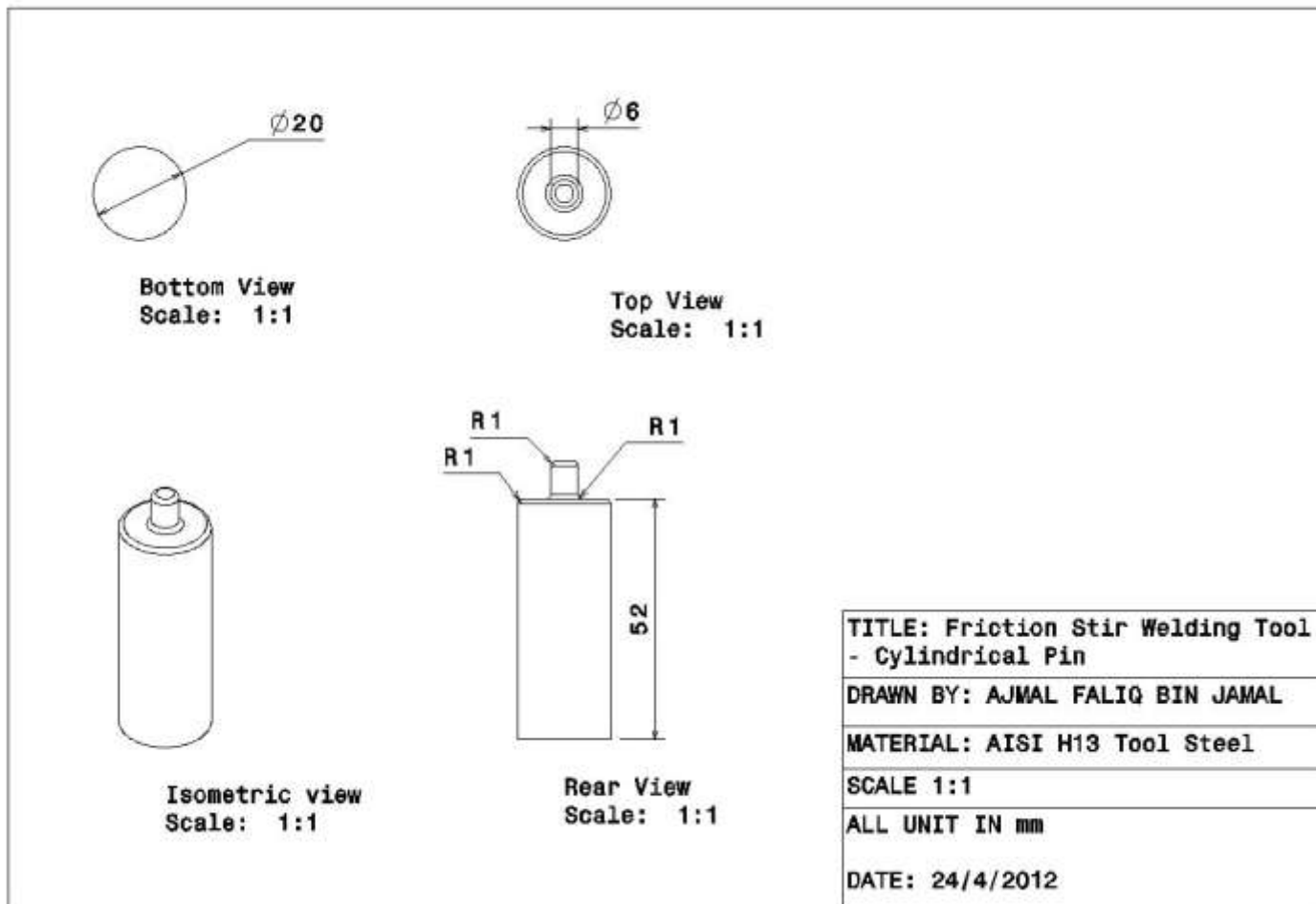
29. Elangovan K Balasubramaniam V, *Influences of pin profile and rotational speed of the tool on the formation of friction stir processing zone in AA 2219 aluminum alloy*, Dept of Manufacturing Engineering, Annamalai University of India (2006).

APPENDICES

Category	Steel
Class	Tool steel
Type	Chromium hot work steel
Designations	France: AFNOR Z 40 COV 5 Germany: DIN 1.2344 Italy: UNI KU Japan: JIS SKD61 Sweden: SS 2242 United Kingdom: B.S. BH 13 United States: ASTM A681 , FED QQ-T-570 , SAE J437 , SAE J438 , SAE J467 , UNS T20813

Table 5.1: AISI H13 Tool Pin Properties and Specification





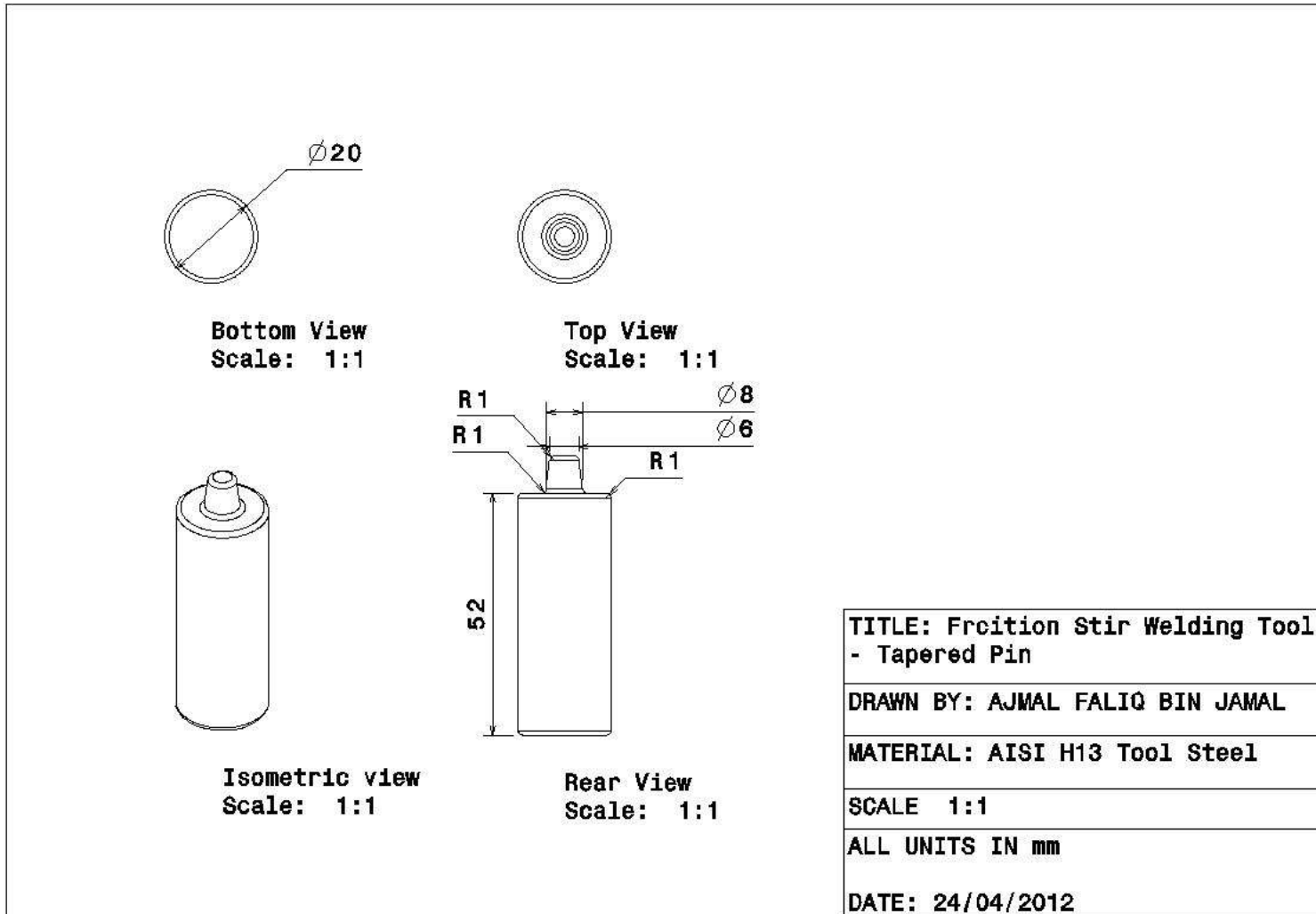




Figure 5.1: CNC Lathe Machine Power Path 15 and the outcome Tool – Tapered and Cylindrical Pin Design



Figure 5.2: Carbolite Heat Treatment Tube Furnace and the end product of the heat treated tool pin



Figure 5.3: 1cm² area of AA6061 (base alloy and weld region) been cut and fitted to the mounting for the purpose of mounting



Figure 5.4: ACM measurement equipment

APPENDIX 7

Current (mA/cm ²)	Potential (mV)	Time (Sec)	Current (mA/cm ²)	Potential (mV)	Time (Sec)
			-0.0047912	-666.93	0
0.0059107	-1096.1	0	-0.0047356	-666.81	0.8750003
0.0048263	-1095.9	1.125	-0.0046962	-666.7	1.5619
0.0041139	-1095.7	1.875	-0.0046739	-666.6	2.312
0.0036903	-1095.6	2.625	-0.0046442	-666.43	3.5619
0.0032306	-1095.4	3.688	-0.0046211	-666.31	4.5
0.0029289	-1095.3	4.563	-0.0045945	-666.15	5.5
0.0026869	-1095.1	5.438	-0.0045839	-666.01	6.4999
0.0022359	-1093.5	6.313	-0.0045947	-665.82	7.437
0.0024347	-1095.2	7.188	-0.0046035	-665.69	8.1249
0.0021476	-1094.7	7.75	-0.0045961	-665.51	9.125
0.0019859	-1094.6	8.625	-0.0045802	-665.34	10.249
0.0018494	-1094.4	9.563	-0.0045576	-665.2	11.186
0.0017984	-1094.6	10.438	-0.0045327	-665.03	12.125
0.001721	-1094.9	11.249	-0.0045062	-664.89	13.061
0.001559	-1094	12.063	-0.0044806	-664.77	14
0.0014795	-1093.9	12.874	-0.0044614	-664.61	14.937
0.0014067	-1093.7	13.688	-0.0044402	-664.45	15.875
0.0013363	-1093.6	14.5	-0.0044162	-664.31	16.875
0.0012719	-1093.5	15.313	-0.0043871	-664.16	17.561
0.0012126	-1093.3	15.813	-0.0043494	-663.97	18.5
0.0011622	-1093.2	16.438	-0.0043285	-663.83	19.499
0.0011105	-1093.1	17.313	-0.0043088	-663.65	20.5
0.0010562	-1092.9	18.188	-0.0042849	-663.54	21.437
0.0010082	-1092.8	19.063	-0.0042686	-663.37	22.436
0.0009632	-1092.7	19.938	-0.0042497	-663.2	23.437
0.0009188	-1092.5	20.749	-0.0042293	-663.05	24.374
0.0008826	-1092.4	21.625	-0.0042114	-662.9	25.375
0.0008448	-1092.3	22.5	-0.0041961	-662.73	26.375
0.0008084	-1092.2	23.375	-0.0041832	-662.61	27.061
0.0007741	-1092	23.938	-0.0041624	-662.41	28
0.0007342	-1091.8	24.813	-0.0041633	-662.27	28.936
0.0005546	-1091.3	25.688	-0.0041574	-662.13	29.875
0.0007165	-1091.6	26.563	-0.0041462	-661.95	30.874
0.0006563	-1091.4	27.438	-0.0041235	-661.81	31.874
0.0006287	-1091.3	28.25			

0.0006063	-1091.2	29.125	-0.0040986	-661.63	32.875
			-0.0040757	-661.48	33.811
0.0005838	-1091	30.063	-0.0040565	-661.35	34.811
0.0006463	-1091.7	30.938	-0.0040383	-661.19	35.812
0.000526	-1090.3	31.813	-0.0040294	-661.02	36.5
0.0005174	-1090.6	32.375	-0.0040317	-660.84	37.437
0.0004374	-1090.4	33.499	-0.0040241	-660.68	38.374
0.0004182	-1090.2	34.375	-0.0040146	-660.56	39.312
0.0004109	-1090.1	35.188	-0.0040291	-660.37	40.312
0.0004065	-1090	36.063	-0.0040526	-660.24	41.311
0.0004042	-1089.8	36.937	-0.0040455	-660.08	42.25
0.000429	-1089.7	37.813	-0.0040387	-659.95	43.186
0.0003749	-1089.6	38.688	-0.0040363	-659.79	44.125
0.0003973	-1089.4	39.5	-0.0040171	-659.67	45.061
0.0003698	-1089.3	40.313	-0.0039961	-659.53	45.687
0.0003747	-1089.2	40.875	-0.003972	-659.32	46.687
0.0003748	-1089	41.75	-0.0039477	-659.17	47.686
0.0003668	-1088.8	42.688	-0.0039153	-659.01	48.625
0.000354	-1088.7	43.563	-0.0039218	-658.84	49.624
0.0003486	-1088.6	44.375	-0.0039222	-658.72	50.625
0.0003502	-1088.4	45.25	-0.0038988	-658.53	51.562
0.0003395	-1088.3	46.125	-0.0038768	-658.38	52.561
0.0003077	-1087.4	47	-0.0038645	-658.25	53.562
0.0003158	-1088.1	47.874	-0.0038525	-658.09	54.499
0.0003176	-1087.9	48.75	-0.003841	-657.93	55.187
0.00031	-1087.8	49.25	-0.0038296	-657.73	56.186
0.0003048	-1087.6	49.813	-0.0038156	-657.57	57.186
0.0003326	-1088.3	50.688	-0.0038121	-657.44	58.125
0.0002638	-1086.9	51.563	-0.0038153	-657.29	59.061
0.0002821	-1087.3	52.375	-0.003818	-657.12	60
0.0002935	-1087.1	53.25	-0.0038096	-656.97	60.936
0.0002641	-1087	54.125	-0.0037931	-656.81	61.875
0.0002713	-1086.8	55	-0.0037769	-656.67	62.875
0.0002568	-1086.7	55.875	-0.0037592	-656.53	63.874
0.0002932	-1086.6	56.688	-0.0037357	-656.35	64.5
0.0002457	-1086.4	57.25	-0.0037093	-656.16	65.499
0.0002447	-1086.3	58.125	-0.0036842	-656.03	66.5
0.0002463	-1086.1	58.938	-0.0036612	-655.87	67.437
0.0002573	-1086	59.813			

0.000228	-1085.9	60.688	-0.0036607	-655.72	68.436
			-0.0036798	-655.56	69.437
0.0002407	-1085.8	61.563	-0.0036989	-655.39	70.374
0.0002266	-1085.6	62.437	-0.0036978	-655.24	71.375
0.00023	-1085.5	63.25	-0.0036717	-655.09	72.375
0.0002296	-1085.3	64.063	-0.0036331	-654.94	73.311
0.0002251	-1085.2	64.938	-0.0035951	-654.78	74
0.0002192	-1085.1	65.5	-0.0035511	-654.61	74.999
0.0002258	-1084.9	66.375	-0.0035149	-654.45	76
0.0002211	-1084.8	67.25	-0.003492	-654.29	76.937
0.0002149	-1084.6	68.063	-0.0034704	-654.15	77.875
0.0002154	-1084.5	68.938	-0.003453	-654.01	78.812
0.0002087	-1084.4	69.813	-0.0034494	-653.86	79.749
0.0002038	-1084.2	70.688	-0.0034352	-653.69	80.687
0.0002033	-1084.1	71.563	-0.0034239	-653.59	81.624
0.0002066	-1084	72.438	-0.0034126	-653.41	82.625
0.0002002	-1083.8	73.249	-0.0033882	-653.26	83.312
0.0002064	-1083.7	73.75	-0.0033611	-653.05	84.25
0.0001925	-1083.6	74.375	-0.0033463	-652.89	85.25
0.0001933	-1083.4	75.25	-0.0033329	-652.76	86.249
0.0002014	-1083.3	76.125	-0.0033384	-652.6	87.187
0.000251	-1083.7	77	-0.0033203	-652.44	88.187
0.0001836	-1083	77.813	-0.0032993	-652.26	89.186
0.0001729	-1082.9	78.625	-0.0032767	-652.13	90.125
0.0001864	-1082.8	79.438	-0.0032519	-652	91.124
0.0001665	-1082.6	80.25	-0.0032468	-651.85	92.125
0.0001449	-1082.5	81.063	-0.0032583	-651.67	92.811
0.00018	-1082.4	81.563	-0.0032925	-651.44	93.75
0.0001671	-1082.3	82.125	-0.0033091	-651.34	94.812
0.0001473	-1082.1	83.125	-0.0033195	-651.16	95.811
0.000163	-1082	84	-0.0033052	-650.99	96.812
0.0001438	-1081.8	84.813	-0.0032888	-650.84	97.812
0.0001718	-1081.7	85.688	-0.0032637	-650.66	98.749
0.0001388	-1081.6	86.563	-0.0032268	-650.53	99.75
0.0001513	-1081.4	87.438	-0.0031965	-650.39	100.74
0.000153	-1081.3	88.313	-0.0031823	-650.21	101.68
0.0001283	-1080.7	89.125	-0.0031694	-650.06	102.37
0.0001397	-1081	89.688	-0.003163	-649.88	103.37
0.0001285	-1080.9	90.563			

0.0001445	-1080.7	91.438	-0.0031479	-649.71	104.37
			-0.0031273	-649.58	105.31
0.0001509	-1080.7	92.313			
			-0.0031138	-649.43	106.25
0.0001469	-1080.4	93.141			
			-0.0031178	-649.28	107.18
0.0001549	-1080.4	93.999			
			-0.0031244	-649.12	108.12
0.0001431	-1080.2	94.875			
			-0.0031258	-648.99	109.06
0.0001406	-1080.1	95.688			
			-0.0031283	-648.82	110.06
0.0001578	-1080.4	96.5			
			-0.0031286	-648.67	111.06
0.0001211	-1080.5	97.313			
			-0.0031261	-648.49	111.74
0.0001243	-1079.7	97.813			
			-0.0031147	-648.32	112.75
0.0001377	-1079.5	98.438			
			-0.003089	-648.16	113.68
0.0001299	-1079.4	99.313			
			-0.003067	-648.03	114.62
0.0001301	-1079.3	100.18			
			-0.0030429	-647.87	115.62
0.0001238	-1079.1	101.07			
			-0.0030228	-647.71	116.62
0.0001297	-1079	101.95			
			-0.0030245	-647.57	117.62
0.0001203	-1078.8	102.76			
			-0.0030263	-647.4	118.56
0.0001324	-1078.7	103.76			
			-0.0030183	-647.23	119.56
0.0001373	-1078.5	104.76			
			-0.0030022	-647.09	120.56
0.0001295	-1078.4	105.57			
			-0.0029624	-646.92	121.24
0.0001219	-1078.3	106.2			
			-0.0029404	-646.76	122.18
0.0001249	-1078.1	107.2			
			-0.0029098	-646.6	123.12
0.0001215	-1077.9	108.4			
			-0.0028799	-646.47	124.06
0.000121	-1077.8	109.34			
			-0.0028538	-646.3	125.06
0.0001226	-1077.6	110.34			
			-0.0028364	-646.15	126.06
0.0000986	-1077	111.54			
			-0.0028377	-645.97	127
0.0001165	-1077.2	112.48			
			-0.0028396	-645.82	127.93
0.0001137	-1077.1	113.48			
			-0.00284	-645.67	128.87
0.0001166	-1077	114.48			
			-0.0028324	-645.54	129.81
0.0001212	-1076.8	115.42			
			-0.0028215	-645.39	130.43
0.0000974	-1076	116.1			
			-0.0028227	-645.22	131.43
0.0001275	-1076.5	117.11			
			-0.0028217	-645.07	132.43
0.0001127	-1076.3	118.11			
			-0.0028019	-644.88	133.37
0.0001055	-1076.1	119.04			
			-0.002763	-644.75	134.37
0.0001047	-1076	119.98			
			-0.0027263	-644.6	135.37
0.0001007	-1075.8	120.92			
			-0.0027141	-644.42	136.31
0.000109	-1075.7	121.86			
			-0.0027083	-644.27	137.31
0.0000991	-1075.6	122.79			
			-0.0027033	-644.09	138.31
0.0001073	-1075.4	123.73			
			-0.0027161	-643.94	139.25
0.0000986	-1075.2	124.73			

0.0001014	-1075.1	125.42	-0.0027325	-643.81	139.93
			-0.0027521	-643.61	140.93
0.0000965	-1074.9	126.42			
			-0.0027533	-643.46	141.93
0.0000954	-1074.8	127.35			
			-0.0027392	-643.33	142.87
0.0000926	-1074.6	128.29			
			-0.0027306	-643.15	143.81
0.0001004	-1074.4	129.29			
			-0.0027312	-643.01	144.75
0.0001008	-1074.3	130.29			
			-0.0027289	-642.85	145.68
0.0000928	-1074.1	131.29			
			-0.0027239	-642.7	146.62
0.0000901	-1073.5	132.23			
			-0.002711	-642.59	147.56
8.20E-05	-1073.8	133.23			
			-0.0027067	-642.43	148.56
8.90E-05	-1073.7	134.23			
			-0.0027045	-642.28	149.25
0.000105	-1073.5	134.92			
			-0.0027005	-642.05	150.18
0.0000904	-1073.3	135.86			
			-0.0026736	-641.92	151.18
8.37E-05	-1073.1	136.79			
			-0.0026387	-641.75	152.18
0.0000931	-1073	137.79			
			-0.0026107	-641.59	153.12
0.0000963	-1072.8	138.79			
			-0.0025839	-641.45	154.12
0.0001065	-1072.7	139.79			
			-0.0025716	-641.31	155.12
0.0000972	-1072.5	140.73			
			-0.0025572	-641.14	156.06
0.0001018	-1072.4	141.73			
			-0.0025458	-640.99	157.06
0.0000917	-1072.2	142.67			
			-0.0025398	-640.85	158.06
0.0000969	-1072	143.61			
			-0.002525	-640.67	158.75
8.12E-05	-1071.9	144.29			
			-0.0025009	-640.48	159.68
8.59E-05	-1071.7	145.29			
			-0.0024769	-640.37	160.62
8.03E-05	-1071.6	146.29			
			-0.0024518	-640.21	161.56
0.0000999	-1071.5	147.23			
			-0.0024258	-640.06	162.56
7.85E-05	-1071.2	148.17			
			-0.0023967	-639.89	163.56
7.63E-05	-1071.1	149.11			
			-0.0023734	-639.73	164.56
0.0000928	-1071	150.04			
			-0.0023537	-639.58	165.5
6.33E-05	-1070.8	150.98			
			-0.0023482	-639.4	166.5
0.0000953	-1070.7	151.92			
			-0.0023429	-639.26	167.49
5.75E-05	-1070.6	152.92			
			-0.0023318	-639.09	168.18
8.83E-05	-1070.4	153.61			
			-0.002329	-638.9	169.12
8.21E-05	-1070.2	154.54			
			-0.0023335	-638.77	170.06
6.01E-05	-1070	155.54			
			-0.0023424	-638.62	170.99
-1.01E-05	-1069.6	158.67			
			-0.0023441	-638.46	171.99

Table 5.2 and 5.3: Data of Polarization Potentiostatic Measurement via ACM Potentiostat (-100 to 100mV range with 10mV/ min reading)